Atmos. Chem. Phys. Discuss., https://doi.org/10.5194/acp-2017-613
Manuscript under review for journal Atmos. Chem. Phys.
Discussion started: 1 August 2017

Atmospheric Chemistry and Physics Discussions

First long-term and near real-time measurement of atmospheric trace elements in Shanghai, China

Yunhua Chang[1, 2], Kan Huang[3], Congrui Deng[3], Zhong Zou[4], Shoudong Liu[1, 2], and Yanlin Zhang[1, 2 *]

[1]Yale-NUIST Center on Atmospheric Environment, International Joint Laboratory on Climate and Environment Change (ILCEC), Nanjing University of Information Science & Technology, Nanjing 210044, China

[2]Key Laboratory of Meteorological Disaster, Ministry of Education (KLME)/ Collaborative Innovation Center on Forecast and Evaluation of Meteorological Disasters (CIC-FEMD), Nanjing University of Information Science & Technology, Nanjing 210044, China

[3]Center for Atmospheric Chemistry Study, Shanghai Key Laboratory of Atmospheric Particle Pollution and Prevention (LAP[3]), Department of Environmental Science and Engineering, Fudan University, Shanghai 200433, China

[4]Pudong New Area Environmental Monitoring Station, Shanghai 200135, China

Correspondence to: Yanlin Zhang (dryanlinzhang@outlook.com or zhangyanlin@nuist.edu.cn)

Abstract: Atmospheric trace elements, especially metal species, are an emerging environmental and health concern with poorly constrained on its abundances and sources in Shanghai, the most important industrial megacity in China. Here we continuously performed a one-year (from March 2016 to February 2017) and hourly-resolved measurement of eighteen elements in fine particles ($PM_{2.5}$) at Shanghai urban center with a Xact multi-metals monitor and several collocated instruments. Independent ICP-MS offline analysis of filter samples was used to validate the performance of Xact that was based on energy-dispersive X-ray fluorescence analysis of aerosol deposits on reactive filter tapes. Mass concentrations (mean±1σ; ng m^{-3}) determined by Xact ranged from detection limits (nominally 0.1 to 20 ng m^{-3}) to 14.7 μg m^{-3}, with Si as the most abundant element (638.7±1004.5), followed by Fe

(406.2±385.2), K (388.6±326.4), Ca (191.5±383.2), Zn (120.3±131.4), Mn (31.7±38.7), Pb (27.2±26.1), Ba (24.2±25.4), V (13.4±14.5), Cu (12.0±11.4), Cd (9.6±3.9), As (6.6±6.6), Ni (6.0±5.4), Cr (4.5±6.1), Ag (3.9±2.6), Se (2.6±2.9), Hg (2.2±1.7), and Au (2.2±3.4). Metal related oxidized species comprised an appreciable fraction of $PM_{2.5}$ during all seasons, accounting for 8.3% on average. As a comparison, atmospheric metal pollution level in Shanghai was comparable with other industrialized cities in East Asia but one or two orders magnitude higher than the sites in North America and Europe. Here our high time-resolution observations over long-term period also offer a unique opportunity to provide robust diurnal profiles for each species, which are useful in determining the sources and processes contributing to the fluctuation of atmospheric trace elements. Besides, various mathematical methods and physical evidences were served as criteria to constrain various solutions of source identification. Results showed that atmospheric trace elements pollution in Shanghai was the interplay of local emissions and regional transport, and different sources of metal species generally have different variation patterns associated with different source regions. Specifically, V and Ni were confirmed as the prominent and exclusive tracer of heavy oil combustion from shipping traffic. Fe and Ba were strongly related to brake wear, and exhibited significant correlation with Si and Ca, suggesting that Si and Ca in Shanghai were primarily sourced from road fugitive dust rather than long-distance dust transport and local building construction sites. Stationary combustion of coal was found to be the major source of As, Se, Pb, Cu and K, and the ratio of As/Se was used to infer that coal consumed in Shanghai likely originated from Henan coal fields in Northern China. Cr, Mn and Zn were the mixed result of emissions from stationary combustion coal, ferrous metals production, and nonferrous metals processing. Ag and Cd in Shanghai urban atmosphere were also the mixture of miscellaneous sources. Collectively, our findings in this study provide baseline data with high detail, which are needed for developing effective control strategies to reduce the high risk of acute exposure to atmospheric trace elements in China's megacities.

Atmos. Chem. Phys. Discuss., https://doi.org/10.5194/acp-2017-613
Manuscript under review for journal Atmos. Chem. Phys.
Discussion started: 1 August 2017

1. Introduction

It has been broadly recognized that personal exposure to atmospheric aerosols have detrimental consequences and aggravating effects on human health such as respiratory, cardiovascular, and allergic disorders (Pope III et al., 2002; Pope III et al., 2009; Shah et al., 2013; West et al., 2016; Burnett et al., 2014). Among the chemical components relevant for aerosol health effects, airborne heavy metals (a very imprecise term without authoritative definition (Duffus John, 2002), loosely refers to elements with atomic density greater than 4.5 g cm^{-3} (Streit, 1991)) are of particular concern as they typically feature with unique properties of bioavailability and bioaccumulation (Morman and Plumlee, 2013; Tchounwou et al., 2012; Fergusson, 1990; Kastury et al., 2017), representing 7 of the 30 hazardous air pollutants identified by the US Environmental Protection Agency (EPA) in terms of posing the greatest potential health threat in urban areas (see www.epa.gov/urban-air-toxics/urban-air-toxic-pollutants). Depending on aerosol composition, extent and time of exposure, previous studies have confirmed that most metal components of fine particles ($PM_{2.5}$; particulate matter with aerodynamic diameter equal to or less than 2.5 μm) exerted a multitude of significant diseases from pulmonary inflammation, to increased heart rate variability, to decreased immune response (Fergusson, 1990; Morman and Plumlee, 2013; Leung et al., 2008; Hu et al., 2012; Pardo et al., 2015; Kim et al., 2016).

Guidelines for atmospheric concentration limits of many trace metals are provided by the World Health Organization (WHO) (WHO, 2005). In urban atmospheres, ambient trace metals typically represent a small fraction of $PM_{2.5}$ on a mass basis, while metal species like Cd, As, Co, Cr, Ni, Pb and Se are considered as human carcinogens even in trace amounts (Iyengar and Woittiez, 1988; Wang et al., 2006; Olujimi et al., 2015). It has been shown that Cu, Cr, Fe and V have several oxidation states that can participate in many atmospheric redox reactions (Litter, 1999; Brandt and van Eldik, 1995; Seigneur and Constantinou, 1995; Rubasinghege et al., 2010a), which can catalyze the generation of reactive oxygenated species (ROS) that have been associated with direct

molecular damage and with the induction of biochemical synthesis pathways (Charrier and Anastasio, 2012; Strak et al., 2012; Rubasinghege et al., 2010b; Saffari et al., 2014; Verma et al., 2010; Jomova and Valko, 2011). Additionally, lighter elements such as Si, Al and Ca are the most abundant crustal elements next to oxygen, which can typically constitute up to 50% of elemental species in remote continental aerosols (Usher et al., 2003; Ridley et al., 2016). These species are usually associated with the impacts of aerosols on respiratory diseases and climate (Usher et al., 2003; Tang et al., 2017).

Health effects of airborne metal species are not only seen from chronic exposure, but also from short-term acute concentration spikes in ambient air (Kloog et al., 2013; Strickland et al., 2016; Huang et al., 2012). In addition, atmospheric emissions, transport, and exposure of trace metals to human receptors may depend upon rapidly evolving meteorological conditions and facility operations (Tchounwou et al., 2012; Holden et al., 2016). Historically accepted ambient trace metals sampling devices generally collect 12 to 24-hr integrated average samples, which are then sent off to be lab analyzed in a time-consuming and labor-intensive way. As a consequence, daily integrated samples inevitably ignore environmental shifts with rapid temporality, and thereby hinder the efforts to obtain accurate source apportionment results such as short-term metal pollution spikes related to local emission sources. In fact, during a short-term trace metals exposure event, 12 or 24-hr averaged sample concentrations for metal species like Pb and As may be orders of magnitude lower than the 4-hr or 15-min average concentration from the same day (Cooper et al., 2010). Current source apportionment studies are mainly performed by statistical multivariate analysis such as receptor models (e.g., Positive Matrix Factorization, PMF), which could greatly benefit from high inter-sample variability in the source contributions through increasing the sampling time resolution. In this regard, continuous monitoring of ambient metal species on a real-time scale is essential in the trace metals sources and their health assessment studies.

Currently, there are only a few devices available for the field sampling of ambient

aerosols with sub-hourly or hourly resolution, i.e., the Streaker sampler, the DRUM (Davis Rotating-drum Unit for Monitoring) sampler, and the SEAS (Semi-continuous Elements in Aerosol Sampler) (Visser et al., 2015b; Visser et al., 2015a; Bukowiecki et al., 2005; Chen et al., 2016). Mass loadings of trace metals collected by these samplers can be analyzed with high sensitive accelerator-based analytical techniques, in particular particle-induced X-ray emission (PIXE) or synchrotron radiation X-ray fluorescence (SR-XRF) (Richard et al., 2010; Bukowiecki et al., 2005; Maenhaut, 2015; Traversi et al., 2014). However, a major drawback of the analysis is that they require a large commitment of analytical time. More recently, aerosol time-of-flight mass spectrometry (Murphy et al., 1998; Gross et al., 2000; DeCarlo et al., 2006), National Institute for Standards and Technology (NIST)-traceable reference aerosol generating method (QAG) (Yanca et al., 2006), distance-based detection motif (Cate et al., 2015), environmental magnetic properties coupled with support vector machine (Li et al., 2017), and Xact^{TM} 625 automated multi-metals analyzer (Fang et al., 2015; Jeong et al., 2016; Phillips-Smith et al., 2017; Cooper et al., 2010) have been developed for more precise, accurate, and frequent measurement of ambient metal species. The Xact method is based on nondestructive XRF analysis of aerosol deposits on reactive filter tapes, which has been validated by US Environmental Technology Verification testing and several other field campaigns (Fang et al., 2015; Phillips-Smith et al., 2017; Jeong et al., 2016; Yanca et al., 2006; Cooper et al., 2010).

Located at the heart of the Yangtze River Delta, Shanghai is home to nearly 25 million people as of 2015, marked as the largest megacity in China (Chang et al., 2016). Shanghai city is one of the main industrial centers of China, playing a vital role in the nation's heavy industries, including but not limited to, steel making, petrochemical engineering, thermal power generation, auto manufacture, aircraft production, and modern shipbuilding (Normile, 2008; Chang et al., 2016; Huang et al., 2011). Besides, Shanghai is China's most important gateway for foreign trade, which has the world's busiest port, handled over 37 million standard containers in 2016 (see www.simic.net.cn/news_show.php?lan=en&id=192101). As a consequence, Shanghai

is potentially subject to substantial quantities of trace metal emissions (Duan and Tan, 2013; Tian et al., 2015). Ambient concentrations of trace metals, especially Pb and Hg, in Shanghai atmospheres have been sporadically reported during the past two decades (Shu et al., 2001; Lu et al., 2008; Wang et al., 2013; Zheng et al., 2004; Huang et al., 2013; Wang et al., 2016). Of current interest are V and Ni, which are often indicative of heavy oil combustion from ocean-going vessels (Fan et al., 2016; Liu et al., 2017). Still, previous work rarely illustrated a full spectrum of metal species in ambient aerosols. Meanwhile, most available source evidences were inferred based on filter sampling and off-line analysis, which were not necessarily representative of actual origins. Furthermore, recent attribution of hospital emergency-room visits in China to $PM_{2.5}$ constituents failed to take short-term variations of trace metals into account (Qiao et al., 2014), which could inevitably underestimate the toxicity of aerosols and potentially misestimate the largest influence of aerosol components on the health effects (Honda et al., 2017).

In this study, the first of its kind, we conducted a long-term and near real-time measurement of atmospheric trace metals in $PM_{2.5}$ with a Xact multi-metals analyzer in Shanghai, China, from March 2016 to February 2017. The primary target of the present study is to elucidate the atmospheric abundances, variation patterns and source contributions of trace elements under complex urban environment, which can be used to support future health studies.

2. Methods

2.1 Field measurements

2.1.1 Site description

Figure 1a shows the map of eastern China with provincial borders and land covers, in which Shanghai city (provincial level) sits in the middle portion of China's eastern coast and its metropolitan area (indicated as densely-populated area in Fig. 1b) concentrated on the south edge of the mouth of the Yangtze River. The municipality borders the

170 provinces of Jiangsu and Zhejiang to the north, south and west, and is bounded to the east by the East China Sea (Fig. 1a). Shanghai has a humid subtropical climate and experiences four distinct seasons. Winters are chilly and damp, with northwesterly winds from Siberia can cause nighttime temperatures to drop below freezing. Air pollution in Shanghai is low compared to other cities in northern China like Beijing, 175 but still substantial by world standards, especially in winter (Han et al., 2015; Chang et al., 2017).

Field measurements were performed at the rooftop (~18 m above ground level) of Pudong Environmental Monitoring Center (PEMC; 121.5447°E, 31.2331°N; ~7 m above sea level) in Pudong New Area of southwestern Shanghai with dense population 180 (Fig. 1b). Pudong New Area is described as the "showpiece" of modern China due to its height-obsessed skyline and export-oriented economy. For PEMC, there were no metal-related sources (excepting for on-road traffic) and high-rise buildings nearby to obstruct observations, and air mass could flow smoothly. More broadly, as indicted in Fig. 1c, PEMC is surrounded by multitudinous emissions sources like coal-fired power 185 plants (CFPP) in its four directions and iron and steel smelting in the northwest. Besides, a large amount of ship exhaust emissions in 2010 such V (Fig. 1d) and Ni (Fig. 1e) in the YRD and the East China Sea within 400 km of China's coastline was recently quantified based on an automatic identification system model (Fan et al., 2016). Therefore, PEMC can be regarded as an ideal urban receptor site of various emission 190 sources. More information regarding the sampling site has been given elsewhere (Chang et al., 2017; Chang et al., 2016).

2.1.2 Hourly elemental species measurements

From March 1st 2016 to February 28th 2017, hourly ambient mass concentrations of eighteen elements (Si, Fe, K, Ca, Zn, Mn, Pb, Ba, V, Cu, Cd, As, Ni, Cr, Ag, Se, Hg, 195 and Au) in $PM_{2.5}$ were determined by a Xact multi-metals monitor (Model Xact™ 625, Cooper Environmental Services LLT, OR, USA) (Phillips-Smith et al., 2017; Jeong et al., 2016; Fang et al., 2015; Yanca et al., 2006). Specifically, the Xact sampled the air

on a reel-to-reel Teflon filter tape through a $PM_{2.5}$ cyclone inlet (Model VSCC-A, BGI Inc., MA, USA) at a flow rate of 16.7 L min^{-1}. The resulted $PM_{2.5}$ deposit on the tape was automatically advanced into the analysis area for nondestructive energy-dispersive X-ray fluorescence analysis to determine the mass of selected elemental species as the next sampling was being initiated on a fresh tape spot. Sampling and analysis were performed continuously and simultaneously, except during advancement of the tape (~20 sec) and during daily automated quality assurance checks. For every event of sample analysis, the Xact included a measurement of pure Pd as an internal standard to automatically adjust the detector energy gain. XRF response was calibrated using thin film standards for each metal element of interest. These standards were provided by the manufacturer of Xact, producing by depositing vapor phase elements on blank Nuclepore (Micromatter Co., Arlington, WA, USA). The Nuclepore filter of known area was weighed before and after the vapor deposition process to determine the concentration (μg cm^{-2}) of each element. In this study, excellent agreement between the measured and standard masses for each element was observed, indicating a deviation of < 5%. The 1-hr time resolution minimum detection limits (in ng m^{-3}) were: Si (17.80), K (1.17), Ca (0.30), V (0.12), Cr (0.12), Mn (0.14), Fe (0.17), Ni (0.10), Cu (0.27), Zn (0.23), As (0.11), Se (0.14), Ag (1.90), Cd (2.50), Au (0.23), Ba (0.39), Hg (0.12), and Pb (0.13).

As a reference method to validate Xact on-line measurements, daily $PM_{2.5}$ samples were also collected at PEMC site using a four-channel aerosol sampler (Tianhong, Wuhan, China) on 47 mm cellulose acetate and glass filters at a flow rate of 16.7 L min^{-1}. The sampler was operated once a week with a 24-hr sampling time (starting from 10:00 am). In total 48 filter samples (21 cellulose acetate filter samples and 27 glass filter samples) were collected, in which 8 paired samples were simultaneously collected by cellulose acetate and glass filters. In the laboratory, elemental analysis procedures were strictly followed the latest national standard method "Ambient air and stationary source emission-Determination of metals in ambient particulate matter-Inductively coupled plasma/mass spectrometry (ICP-MS)" (HJ 657-2013) issued by the Chinese Ministry

of Environmental Protection. A total of 24 elements (Al, Fe, Mn, Mg, Mo, Ti, Sc, Na, Ba, Sr, Sb, Ca, Co, Ni, Cu, Ge, Pb, P, K, Zn, Cd, V, S, and As) were measured using an Inductively coupled plasma-mass spectrometry (ICP-MS; Agilent, CA, USA). The results of the 8 paired samples were compared firstly. Significant correlations were observed for species of K, Cr, Mn, Fe, Ni, Cu, As, Cd, Ba, Zn, and Pb (Table S1), and these species were used to validate the performance of Xact. In Table S1, the slope values of Cr (1.9) and Ba (2.6) were higher than other species, this can be explained by higher background values of Cr and Ba collected by cellulose acetate filters.

2.1.3 Auxiliary measurements, quality assurance and quality control

Hourly mass concentrations of $PM_{2.5}$ were measured using a Thermo Fisher Scientific TEOM 1405-D. Data on hourly concentrations of CO, NO_2, and SO_2 were provided by PEMC. Meteorological data, including ambient temperature (*T*), relative humidity (RH), wind direction (WD) and wind speed (WS), were provided by Shanghai Meteorological Bureau at Century Park station (located approximately 2 km away from PEMC). All the above online measurement results were averaged to a 1 hr resolution.

As data in the current study were collected in near-real time, the importance for quality assurance and quality control (QA/QC) system can be crucial in order to improve data quality throughput. The routine procedures, including the daily zero/standard calibration, span and range check, station environmental control, and staff certification, were followed the Technical Guideline of Automatic Stations of Ambient Air Quality in Shanghai based on the national specification HJ/T193–2005, which was modified from the technical guidance established by the USEPA. QA/QC for the Xact measurements was implemented throughout the campaign. The internal Pd, Cr, Pb, and Cd upscale values were recorded after the instrument's daily programmed test, and the PM_{10} and $PM_{2.5}$ cyclones were cleaned weekly.

2.2 Data analysis

2.2.1 Statistical analysis

To identify possible sources of measured trace metals, three methods of statistical analysis, i.e., correlation matrix, principle component analysis (PCA), and hierarchical clustering of reordering correlation matrix, were performed. The "corrplot" package in R is a graphical display of a correlation matrix, confidence interval. It also contains specific algorithms to do matrix. More information regarding corrplot can be found at CRAN.R-project.org/package=corrplot (Wei and Simko, 2016).

Spearman correlations were firstly performed to establish correlations between trace metals, which can be used to investigate the dependence among multiple metal species at the same time. The result is a table containing the correlation coefficients between each variable and the distribution of each metal species on the diagonal. Secondly, principle component analysis (PCA) with a varimax rotation (SPSS Statistics® 24, IBM®, Chicago, IL, USA) was performed on the measured data set, which have been used widely in receptor modelling to identify major source categories. The technique operates on sample-to-sample fluctuations of the normalized concentrations. It does not directly yield concentrations of species from various sources but identifies a minimum number of common factors for which the variance often accounts for most of the variance of species (e.g., (Venter et al., 2017), and references therein). The trace metal concentrations determined for the 18 species were subjected to multivariate analysis of Box-Cox transformation and varimax rotation, followed by subsequent PCA. Lastly, we applied agglomeration strategy for hierarchical clustering, a method of cluster analysis which seeks to build a hierarchy of clusters, to mining the hidden structure and pattern in the correlation matrix (Murdoch and Chow, 1996; Friendly, 2002). In order to decide which clusters should be combined as a source, or where a cluster should be split, a measure of dissimilarity between sets of observations is required, Ward's method is served as a criterion applied in hierarchical cluster analysis. The "corrplot" package can draw rectangles around the chart of correlation matrix (indicated as a potential source) based on the results of hierarchical clustering.

2.2.2 Conditional probability function and bivariate polar plot for tracing source

Atmos. Chem. Phys. Discuss., https://doi.org/10.5194/acp-2017-613
Manuscript under review for journal Atmos. Chem. Phys.
Discussion started: 1 August 2017

regions

The determination of the geographical origins of trace metals in Shanghai requires the use of diagnostic tools such as conditional probability function (CPF) and bivariate polar plot (BPP), which are very useful in terms of quickly gaining an idea of source impacts from various wind directions and have already been successfully applied to various atmospheric pollutants and pollution sources (Chang et al., 2017; Carslaw and Ropkins, 2012). In this study, the CPF and BPP were performed on the one-year data set for the major trace metals with similar source. The two methods have been made in the R "openair" package and are freely available at www.openair-project.org (Carslaw and Ropkins, 2012).

The CPF is defined as CPF = m_θ/n_θ, where m_θ is the number of samples in the wind sector θ with mass concentrations greater than a predetermined threshold criterion, and n_θ is the total number of samples in the same wind sector. CPF analysis is capable to show which wind directions are dominated by high concentrations and give the probability of doing so. In this study, 90th percentile of a given metal species was set as threshold, and 24 wind sectors were used ($\Delta\theta = 15^0$). Calm wind (< 1 m s^{-1}) periods were excluded from this analysis due to the isotropic behavior of wind vane under calm winds.

The BPP demonstrate how the concentration of a targeted species varies synergistically with wind direction and wind speed in polar coordinates, which thus is essentially a non-parametric wind regression model to alternatively display pollution roses but include some additional enhancements. These enhancements include: plots are shown as a continuous surface and surfaces are calculated through modelling using smoothing techniques. These plots are not entirely new as others have considered the joint wind speed-direction dependence of concentrations (see for example Liu et al. (2015)). However, plotting the data in polar coordinates and for the purposes of source identification is new. The BPP has described in more detail in Carslaw et al. (2006) and the construction of BPP had been presented in our previous work (Chang et al., 2017).

3 Results and discussion

3.1 Mass concentrations

3.1.1 Data overview and comparison

The temporal patterns and summary statistics of hourly elemental species concentrations determined by the Xact at PEMC during March 2016-Feburary 2017 are reported in Fig. 2. The mass concentrations of 18 elements measured in Shanghai were sorted from high to low in Fig. 3. The one-year data set presented in the current study, to the best of our knowledge, represents the longest on-line continuous measurement series of atmospheric trace metals.

Taking the study period as a whole, ambient average mass concentrations of elemental species varied between detection limit (ranging from 0.05 to 20 ng m^{-3}) and nearly 15 μg m^{-3}, with Si as the most abundant element (mean ± 1σ; 638.7 ± 1004.5 ng m^{-3}), followed by Fe (406.2 ± 385.2 ng m^{-3}), K (388.6 ± 326.4 ng m^{-3}), Ca (191.5 ± 383.2) ng m^{-3}, Zn (120.3 ± 131.4 ng m^{-3}), Mn (31.7 ± 38.7 ng m^{-3}), Pb (27.2 ± 26.1 ng m^{-3}), Ba (24.2 ± 25.4 ng m^{-3}), V (13.4 ± 14.5 ng m^{-3}), Cu (12.0 ± 11.4 ng m^{-3}), Cd (9.6 ± 3.9 ng m^{-3}), As (6.6 ± 6.6 ng m^{-3}), Ni (6.0 ± 5.4 ng m^{-3}), Cr (4.5 ± 6.1 ng m^{-3}), Ag (3.9 ± 2.6 ng m^{-3}), Se (2.6 ± 2.9 ng m^{-3}), Hg (2.2 ± 1.7 ng m^{-3}), and Au (2.2 ± 3.4 ng m^{-3}). According to the ambient air quality standards of China (GB 3095-2012), EU (DIRECTIVE 2004/107/EC) and WHO, the atmospheric concentration limits for Cd, Hg, As, Cr (VI), Mn, V, and Ni are 5, 50 (1000 for WHO), 6 (6.6 for WHO), 0.025, 150 (WHO), 1000 (WHO), and 20 (25 for WHO) ng m^{-3}, respectively. Therefore, airborne metals pollution in Shanghai is generally low by the current limit ceilings. Nevertheless, information regarding the specific metal compounds or chemical forms is rarely available given that most analytical techniques only record data on total metal content. In the absence of this type of information, it is generally assumed that many of the elements of anthropogenic origin (especially from combustion sources) are present in the atmosphere as oxides. Here we reconstructed the average mass concentrations of

metal and crustal oxides as 5.2, 5.0, 2.8, and 3.1 μg m^{-3} in spring, summer, fall, and winter, respectively, with the annual average concentration was 3.9 μg m^{-3}, which accounting for 8.3% of total $PM_{2.5}$ mass (47 μg m^{-3}) in 2016. Detailed calculation of the reconstructed mass has been fully described elsewhere (Dabek-Zlotorzynska et al., 2011).

The toxicological effect of hazardous metal species is more evident and well aware in soils and aquatic ecosystems, while few (if any) studies on the geochemical cycle of trace metals have considered the fast dynamics of trace metals in the atmosphere. Using a diversity of chemical, physical, and optical techniques, elevated atmospheric concentrations of various metal species have been observed globally; however, a tiny minority of them were performed in a way of high time-resolved. As a comparison, we compiled previous work related to the near real-time measurements of trace metals concentrations in Table 1. The concentrations of most trace metals in Shanghai were commonly an order or two orders of magnitude higher than the sites measured in Europe and North America, while generally ranged in the same level as industrialized city like Kwangju in South Korea. Exceptionally, the concentrations of V and Ni in Shanghai were up to three times higher than that of Kwangju City. This can be expected since Shanghai has the world's busiest container port, and V and Ni were substantially and almost exclusively emitted from heavy oil combustion in ship engines of ocean-going vessels (see more discussion in Section 3.2 and 3.3).

3.1.2 Variations at multiple time scales

In contrast to traditional trace metals measurements, the on-line XRF used in the current study enables measurement of metal species concentrations with 1 hr resolution, which are useful both for source discrimination and in determining the processes contributing to elevated trace metals levels through investigation of their diurnal cycles. We will also discuss weekly cycles because certain emission sources may make a pause or reduction during weekends. Additionally, Shanghai has a humid subtropical climate and experiences four distinct seasons, which could potentially exert an influence on the

mass concentrations of atmospheric metal species. Therefore, monthly and seasonal variations of ambient concentrations for each metal species were demonstrated. The variations of weather data, including *T*, RH, wind speed, wind direction, and precipitation, at PEMC during our study period were also illustrated in Fig. S1.

As depicted in Fig. 4, the seasonal-averaged mass concentrations of Ag and Cd stayed exceptionally constant regardless of the season. Moreover, variations of Ag and Cd in Fig. 5 are highly consistent at weekly and diurnal basis, both exhibiting a sharp increase of (normalized) mass concentrations after midnight and then an outright decline after 1:00 (local time), and keeping quite steady during the rest of the day. Globally, anthropogenic emissions of Ag and Cd exceed the natural rates by well over an order of magnitude. Thus, our results strongly signaled that Ag and Cd pollution in highly populous Shanghai had very stable and climate-independent anthropogenic emission sources.

Except for Ag and Cd, other metal species were seasonally variable without a uniform variation pattern (Fig. 4). Specifically, the concentrations of five metal species, i.e., As, Cu, Hg, K, and Pb, were higher in winter and lower in summer, which were consistent with the seasonal variation pattern of aerosol organics, sulphate, nitrate, and ammonium that were fully-explored in China. Generally, severer air pollution in Eastern China during winter were mainly attributed to the accumulation of pollutants emitted from coal-based heating in conjunction with stagnant meteorological conditions (Huang et al., 2013). However, more trace metals like Ba, Cr, Fe, Mn, Ni, V, and Zn shown the highest concentrations in spring, suggesting more complex sources and different physical/chemical formations of atmospheric metal species in Shanghai (see discussion later). A better example is Ca and Si, which presented the highest degree of seasonal variations with higher concentration levels in summer.

Like Ag and Cd, another example of covariation is V and Ni (Fig. 6). Diurnally, both V and Ni peaked at around 6:00 and then gradually decreased to the bottom at 14:00, which were generally in accord with wind speed (Fig. 6c), suggesting that V- and Ni-

containing aerosols in Shanghai undergo mid- to long-range atmospheric transport. Co-emitted from heavy oil combustion, previous studies in Shanghai port have concluded that a ratio of 3.4 for V/Ni in ambient aerosols could be a reliable indicator of ship traffic source. Here performed in urban area, the average ratio of V/Ni in our study was 3.1 with slightly seasonal changes (Fig. 7), which was very close to the ratio of averaged V and Ni content in ship heavy fuel oils, indicating V- and Ni-containing aerosols subject to minor atmospheric transformation and thus can be served as a robust tracer of shipping emissions even in costal urban areas. The office hours for Shanghai customs is Monday through Saturday, and the most important holiday in the Chinese Calendar-Lunar New Year-is usually celebrated during February. This can be used to explain that the weekly (monthly) lowest impact of shipping emissions in Shanghai was occurred during Sunday (Fig. 6c) (February (Fig. 6d)).

Distinctive diurnal variation patterns are observed for Si, Ca, Fe, Ba (Fig. 8) as well as Mn and Zn (Fig. 9), characterizing by two marked peaks at noon (10:00-11:00) and evening (17:00-18:00), and agreeing well with the diurnal variation of Shanghai traffic flow. Indeed, as the largest megacity in terms of economy and population in China, the contribution of vehicles, both exhaust and non-exhaust emissions (Thorpe and Harrison, 2008), to ambient trace metals cannot to be belittled in Shanghai. As demonstrated in Fig. 8d and Fig. 9d, there is an evident drop in the concentrations of Si, Ca, Fe, Ba, Mn and Zn after entering weekends. Data collected from Shanghai Traffic Administration Bureau, Fig. S2 shows seasonally average weekly cycles of on-road traffic flow in Shanghai, in which the average traffic flows in weekends were lower than that in weekdays. Given that Fe is the support material for brake pad, and the agents present in brake linings typically consist of Zn, Mn and Ba, less traffic flow in weekends not only lower road suspend dust but also cut metal species emissions from brake wear (Zhao et al., 2015; Xie et al., 2008). Nevertheless, monthly variation pattern of Ca was different from other metals during April through July (Fig. 10c), and Si exhibited unusually high levels in July (Fig. 8c) and 1:00 (Fig. 8b). PMF analysis of elemental species has suggested that Fe and Ba in urban atmospheres were primarily caused by

vehicular brake wear while high levels of Si and Ca were more likely driven by road resuspended dust (Heo et al., 2009; Harrison et al., 2012; Jeong et al., 2016; Amato et al., 2011; Xie et al., 2008). Besides, construction activities are always thriving in China, which have been confirmed as an important source of Si- and Ca-rich crustal matters (Tian et al., 2015). Building construction activities in Shanghai are concentrated between the end of spring festival (normally the end of February) and the approach of midsummer heat (August) (Tian et al., 2015). For an annual mean of 16.1 °C, Shanghai averages 28.3 °C in August, and the municipal authority will impose a mandatory moratorium toward outdoor construction once temperature rises to 37 °C (Chang et al., 2016). Besides, heavy-duty diesel vehicles (mostly for transforming and dumping construction waste) in Shanghai can only be allowed to operate after midnight (Chang et al., 2016), leading to some higher emissions from diesel engines and unpaved roads.

In Fig. 10 and Fig. 11, diurnal variations of trace metals like Cu, K, Se, As, Pb, Au, and Hg are seemingly full of clutter. Interestingly however, the monthly and weekly cycles of the above-mentioned metal species are remarkably consistent, hinting at the possibility of sharing similar sources. Apart from anthropogenic activity, the planetary boundary layer height in Shanghai normally reaches its annual climax during August and September (Chang et al., 2016), which are favorable to the vertical dispersion of air pollutants, leading to the lowest concentration levels in Fig. 10. From a perspective of man-made emissions, coal combustion of industrial boilers and nonferrous metal smelting represent the dominant sources for Se/As/Pb/Cr, and Au/Hg, respectively. For Cu, China annually emits around 10000 metric tons Cu, which have long been thought to be primarily sourced from automotive braking because copper or brass is a major ingredient in friction material (Tian et al., 2015). However, our results based on field measurements in Shanghai go against the inherent notion of Cu origins. Gathering evidences have shown that topsoil and coal ash are also enriched in K (Schlosser, et al., 2002; Thompson and Argent, 1999; Westberg et al., 2003; Reff et al., 2009). These findings suggest more diverse sources of trace metals in a highly industrialized megacity like Shanghai.

Atmos. Chem. Phys. Discuss., https://doi.org/10.5194/acp-2017-613
Manuscript under review for journal Atmos. Chem. Phys.
Discussion started: 1 August 2017

3.2 Source analysis

The goal of source analysis in the current study is twofold. On the one hand, we will use various mathematical and physical criteria to constrain various solutions of source apportionment. On the other hand, we will take CPF and BPP as diagnostic tools for quickly gaining the idea of potential source regions, which in turn will contribute to further analysis of source apportionment.

3.2.1 Pinpoint the best possible source

As the first approach in the source analysis, Spearman correlation matrixes were prepared for all measured elemental species and presented in Fig. 12. From Fig. 12, relatively good correlations are observed between trace metals associated with heavy oil combustion (i.e., V and Ni), brake and tire wear (e.g., Fe, Mn, Ba and Zn), trace crustal matters (i.e., Si and Ca), and coal combustion (e.g., Se, As and Pb), indicating the complex influence of multiple sources in Shanghai. Still, trace crustal matters are also well correlated with metal species related to brake and tire wear. As discussed in Section 3.1, the bimodal variations of Si and Ca are also evident, which jointly suggest that the trace crustal matters we observed in Shanghai urban atmosphere were primarily derived from road fugitive dust. Nevertheless, with approximately 70% of most of the airborne crustal species being present in the coarse size fraction (Huang et al., 2013), here we call for more size-resolved sampling and analysis of PM to provide a paramount view of atmospheric trace metals in the future.

Using multiple lines of evidence above, we've inferred heavy oil combustion from ship engines as the possible source of V and Ni. Here in Fig. 12, different from all other inter-correlated trace metals, V and Ni are not only highly correlated but also exclusively correlated to each other. For metal species data greater than their 90th percentile, CPF analysis in Fig. 13 shows that over 90% Ni and almost all V observed in our receptor site come from the west (East China Sea). From a perspective of geographical origin, Fig. 13 also clearly shows major air masses containing both V and

Ni are sourced from the southwest. Collectively, it can be safely concluded that shipping emissions are best possible source of V and Ni in Shanghai. The successful identification of the best possible source, i.e., shipping emissions, is helpful in terms of examining the feasibility of various source apportionment solutions. In other words, V and Ni should be clustered as a single factor/source in any solution.

3.2.2 Explore and constrain more sources

To determine sources of more trace metals, PCA was applied as an exploratory tool, since much larger datasets are required for definitive source apportionment with PCA. Therefore, only the most apparent groupings of metal species relating to expected sources in the region were identified. The factor loadings are presented in Fig. 14, indicating four statistically significant factors with eigenvalues equal to or greater than 1. These four factors obtained explained nearly 80% of the variance. Unexpectedly, PCA of the 18 elemental species did not reveal any meaningful factors. This can be preliminarily tested by the large contribution of V and Ni in two different factors, but more importantly, was attributed to the large influence of nonferrous smelting, coal combustion, and traffic-related emissions on ambient trace metals measured at PEMC (see discussion later).

Matrix reorder in conjunction with clustering analysis can be a powerful tool for mining the hidden structure and pattern in the correlation matrix of Fig. 12. Here six solutions of source apportionment, from 3 sources/factors to 8 sources/sources, determined by clustering analysis were presented in Fig. 15. As mentioned above, we can rule out the solution of 3 and 4 sources/factors in Fig. 15a and 15b at first since V and Ni are combined with Au and Hg as a single source.

In Fig. 15c through 15f, Au and Hg are always clustered together as an individual factor, suggesting certain similar source(s) they may share. Globally, anthropogenic sources, including a large number of industrial point sources, annually account for 2320 Mg of Hg released to the atmosphere (Nriagu, 1996). Despite varied in emission quantity

among different studies, Hg emissions from nonferrous metals production, coal consumption by industrial boilers and coal combustion by power plants incontrovertibly represent the top three anthropogenic sources in China, with a share of 33.1, 25.4 and 20.7% for each sector according to Tian et al. (2015). In other words, stationary combustion of coal contributes roughly half Hg emissions of anthropogenic origins. The distribution of metal-related factories is illustrated in Fig. 1, in which coal-fired power plants encompass our site at every major direction while nonferrous metal-related works are concentrated in the west (especially in the northwest) but absent in the east of PEMC. Here we calculate percentile concentration levels of Au and Hg, and plots them by wind direction in Fig. 16a and 16b, respectively. It is clearly shows Au and Hg are primarily derived from stationary combustion of coal because the overwhelmingly prevailing air masses from the west of PEMC. Even though, there are few 99-99.9th percentile data that are originated from the northwest of PEMC (Fig. 16a and 16b), signaling that nonferrous metals production only affect high percentile concentrations of Au and Hg at PEMC.

Statistically, the relatively weak correlation between Ag and Cd (Fig. 12) denies the possibility that they could equally share the same source. Therefore, the solution of 5 factors/sources illustrated in Fig. 15c is superficially invalid. Knowledge gap remains regarding the emissions of Ag in China, while this is not the case for Cd. Totally 456 metric tons in 2010, the major category sources for Cd emissions in China were nonferrous metals smelting (mainly primary Cu smelting industry), coal consumption by industrial boilers and other non-coal sources, which accounted for 44.0, 22.8 and 8.4% of the total emissions, respectively (Tian et al., 2015). Significantly high concentrations of Ag were also observed near the field of nonferrous metals processing works and coal-fired power plants in China, suggesting that nonferrous metals production and industrial coal consumption are also important source of Ag. As reported in Fig. 16c and 16d, the receptor site, PEMC, evenly receives air masses containing Ag and Cd in all directions, indicating that both Ag and Cd in Shanghai urban atmosphere are the mixture of miscellaneous sources.

Among the reaming metal species, Cu/K/Pb/As/Se, Cr/Mn/Zn, Fe/Ba, and Ca/Si are grouped together as a population from first to last in Fig. 15. In China, 73% of As, 62% Se, 56% of Pb, and 50% Cu emissions were found to be coal combustion (Tian et al., 2015). Therefore, As and Se are typically treated as the specific tracers of coal-related emissions in China (Tian et al., 2015; Zhang, 2010; Ren, 2006). Broadly, different coal field has starkly different contents of As and Se, which offers opportunity to infer the possible region of coal production. For example, the average As content in coal of northern China (0.4-10 mg kg^{-1}) and southern China (0.5-25 mg kg^{-1}) are 3 mg kg^{-1} and 10 mg kg^{-1}, respectively (Zhang, 2010; Ren, 2006). With an average value of 2 mg kg^{-1}, Se content in various Chinese coal fields ranges from 0.1 mg kg^{-1} to 13 mg kg^{-1} (Zhang, 2010; Ren, 2006). We have no direct information regarding As and Se contents in coal that used in Shanghai. As an alternative, here the average ratio of ambient As and Se (As/Se ratio) in Shanghai was calculated as 2.65, which was very close to the As/Se ratio (2.76) in coal (long flame coal of Jurassic period) of Henan Province in northern China (Zhang, 2010). Note that the As/Se ratios in Shanxi Province, a major coal production region in China, are ranged from is 0.24 in Taiyuan (the capital city of Shanxi) to 1.96 in Datong (a prefecture-level city in northern Shanxi) (Zhang, 2010). The emission source regions of Cu, K, Pb, As, and Se are demonstrated in Fig. 17, in which all species are generally transported from far western Shanghai (where stationary combustion of coal located; Fig. 1) to our sampling site.

It is well known that Ca and Si are two of the five most abundant elements in the Earth's crust, enjoying a long reputation of being the most specific tracer of wind-blown dust. Located on the eastern coast of China, Shanghai rarely receives long-range transport of crustal matters from aeolian dust and Gobi deserts in northwestern China (Huang et al., 2013). Sampling in the east side of Shanghai, a majority of measured Ca and Si must be sourced from road fugitive dust or urban construction sites, which can be further validated by the CPF and BPP analysis of Ca and Si (Fig. S3). As discussed above, ambient Fe and Ba at PEMC are strongly associated with brake wear (Zhao et al., 2015). In Fig. 15, significant correlations are observed among Ca, Si, Fe, and Ba, suggesting

that the measured Ca and Si during our study period were more likely derived from road fugitive dust.

As a group of tightly-linked metal species, identifying a principle source for measured Cr, Mn and Zn at PEMC is a daunting task. Cr, Mn and Zn have relatively good correlation with two groups of metal species, i.e., coal combustion-related emissions (i.e., Cu, K, Pb, As, and Se) and brake wear-related emissions (i.e., Fe and Ba). This is basically attributed to the diverse sources of Cr, Mn and Zn themselves in China. For Cr, the national atmospheric emissions from anthropogenic sources in 2010 reached 7465.2 metric tons, of which about 5317.6 metric tons were emitted from coal consumption by industrial boilers (Tian et al., 2015). Coal combustion is also the dominant source of Mn in a national dimension, while in urban areas with intensive road network, the contribution of brake and tire wear to ambient Mn is appreciable. Different from Cr and Mn, ferrous metals smelting sector (31.3%), especially the pig iron and steel production industry, is the leading contributor to Zn emissions in China, followed by coal combustion (21.7%) and nonferrous metals smelting sector (19.3%). The Baosteel company in Shanghai, located in the northwest of PEMC (approximately 20 km apart; Fig. 1), is a flagship manufacturer in terms of producing the first-chop iron and steel throughout China. Fig. S4 also evidently reflect high concentrations of Zn can be occurred in the northwest of PEMC. In sum, ambient Cr, Mn and Zn in Shanghai urban atmosphere is highly mixed with coal combustion by industry sectors and power plants, ferrous metals production, and nonferrous metals smelting.

4. Conclusion and outlook

This paper presents the results from a year-long, near real-time measurement study of 18 trace elements (Si, Fe, K, Ca, Zn, Mn, Pb, Ba, V, Cu, Cd, As, Ni, Cr, Ag, Se, Hg, and Au) in $PM_{2.5}$ using a Xact multi-metal monitor, conducted at an urban site in Shanghai from March 2016 to February 2017. The scientific significance of this work can be reflected by the general findings as follows:

-The Xact multi-metals monitor was demonstrated as a valuable and practical tool for ambient monitoring of atmospheric trace elements through comparing online monitoring results with ICP analyses of offline filter samples.

-The metal concentrations in Shanghai are one or two orders of magnitude higher than in north America and Europe, highlighting the need to allocate more scientific, technical, and legal resources on controlling metals' emissions in China.

-The total of metal related species comprised approximately 8.3% of the $PM_{2.5}$ mass, which should not be ignored in China's recent epidemiologic study of attributing hospital emergency-room visits to $PM_{2.5}$ chemical constituents.

-The full coverage of trace elemental species (18) measurement and the high temporal frequency (hourly) in the work provided unprecedented details regarding the temporal evolution of metal pollution and its potential sources in Shanghai.

-Various mathematical methods (e.g., correlation matrix, hierarchical clustering, and conditional probability function) and physical evidences were used to infer the contribution of local emissions (specific sectors) and long-range transport to measured metal species.

A greater value and more interesting topic to the scientific community would be to fully assess the role of $PM_{2.5}$ chemical constituents (including metal species) and sources of emission to human health. Looking into the future, three major moves will be taken toward thoroughly addressing these questions. Firstly, characterizing the chemical and isotopic (including metal species) signatures of emission sources will be intensively taken through field samplings as well as laboratory simulations (see example of Geagea et al. (2007)). Secondly, Xact multi-metals monitor, Sunset OC/EC analyzer (Chang et al., 2017), and MARGA (Monitoring of AeRosols and Gases) platform will be collocated across a rural-urban-background transect to simultaneous measurement of hourly metal species, carbonaceous aerosols, and inorganic aerosol components in $PM_{2.5}$. Lastly, integrating all available information regarding $PM_{2.5}$ chemical species

and isotopes into receptor model or atmospheric chemical transport model to create more specific and confident source apportionment results.

Competing interests

The authors declare that they have no competing interests.

Data availability

Data are available from the corresponding authors on request.

Acknowledgements

This study was supported by the National Key Research and Development Program of China (2017YFC0210101), Provincial Science Foundation of Jiangsu (Grant no. BK20170946), University Science Research Project of Jiangsu Province (17KJB170011), National Science Foundation of China (Grant nos. 91644103, 41603104, 41429501, and 91644105). Yunhua Chang and Zhong Zou acknowledge the support of the Start-up Foundation for Introducing Talent to NUIST and Shanghai Pudong New Area Sci-tech Development Funds (Grant no. PKJ2016-C01), respectively. We also acknowledge the Qingyue Open Environmental Data Centre (http://data.epmap.org) for the unconditional help in terms of providing criteria pollutants monitoring data.

Reference

Amato, F., Pandolfi, M., Moreno, T., Furger, M., Pey, J., Alastuey, A., Bukowiecki, N., Prevot, A. S. H., Baltensperger, U., and Querol, X.: Sources and variability of inhalable road dust particles in three European cities, Atmos. Environ., 45, 6777-6787, doi: 10.1016/j.atmosenv.2011.06.003, 2011.

Brandt, C. and van Eldik, R.: Transition metal-catalyzed oxidation of sulfur (IV) oxides. Atmospheric-relevant processes and mechanisms, Chem. Rev., 95, 119-190, doi: 10.1021/cr00033a006, 1995.

Bukowiecki, N., Hill, M., Gehrig, R., Zwicky, C. N., Lienemann, P., Hegedüs, F., Falkenberg, G., Weingartner, E., and Baltensperger, U.: Trace metals in ambient air: Hourly size-segregated mass concentrations determined by synchrotron-XRF, Environ. Sci. Technol., 39, 5754-5762, doi: 10.1021/es048089m, 2005.

Burnett, R. T., Pope, C. A., III, Ezzati, M., Olives, C., Lim, S. S., Mehta, S., Shin, H. H., Singh, G., Hubbell, B., Brauer, M., Anderson, H. R., Smith, K. R., Balmes, J. R., Bruce, N. G., Kan, H., Laden, F., Pruss-Ustun, A., Turner, M. C., Gapstur, S.

M., Diver, W. R., and Cohen, A.: An integrated risk function for estimating the global burden of disease attributable to ambient fine particulate matter exposure, Environ. Health. Perspect., 122, 397-403, doi: 10.1289/ehp.1307049, 2014.

Carslaw, D. C., Beevers, S. D., Ropkins, K., and Bell, M. C.: Detecting and quantifying aircraft and other on-airport contributions to ambient nitrogen oxides in the vicinity of a large international airport, Atmos. Environ., 40, 5424-5434, doi: 10.1016/j.atmosenv.2006.04.062, 2006.

Carslaw, D. C. and Ropkins, K.: Openair - An R package for air quality data analysis, Environ. Modell. Softw., 27–28, 52-61, doi: 10.1016/j.envsoft.2011.09.008, 2012.

Cate, D. M., Noblitt, S. D., Volckens, J., and Henry, C. S.: Multiplexed paper analytical device for quantification of metals using distance-based detection, Lab Chip, 15, 2808-2818, doi: 10.1039/c5lc00364d, 2015.

Chang, Y., Zou, Z., Deng, C., Huang, K., Collett, J. L., Lin, J., and Zhuang, G.: The importance of vehicle emissions as a source of atmospheric ammonia in the megacity of Shanghai, Atmos. Chem. Phys., 16, 3577-3594, doi: 10.5194/acp-16-3577-2016, 2016.

Chang, Y., Deng, C., Cao, F., Cao, C., Zou, Z., Liu, S., Lee, X., Li, J., Zhang, G., and Zhang, Y.: Assessment of carbonaceous aerosols in Shanghai, China: Long-term evolution, seasonal variations and meteorological effects, Atmos. Chem. Phys. Discuss., 2017, 1-46, doi: 10.5194/acp-2017-50, 2017.

Charrier, J. G. and Anastasio, C.: On dithiothreitol (DTT) as a measure of oxidative potential for ambient particles: evidence for the importance of soluble transition metals, Atmos. Chem. Phys., 12, 9321-9333, doi: 10.5194/acp-12-9321-2012, 2012.

Chen, B., Stein, A. F., Castell, N., Gonzalez-Castanedo, Y., Sanchez de la Campa, A. M., and de la Rosa, J. D.: Modeling and evaluation of urban pollution events of atmospheric heavy metals from a large Cu-smelter, Sci. Total Environ., 539, 17-25, doi: 10.1016/j.scitotenv.2015.08.117, 2016.

Cooper, J. A., Petterson, K., Geiger, A., Siemers, A., and Rupprecht, B.: Guide for developing a multi-metals, fenceline monitoring plan for fugitive emissions using X-ray based monitors, Cooper Environmental Services, Portland, Oregon, 1-42, 2010.

Dabek-Zlotorzynska, E., Dann, T. F., Kalyani Martinelango, P., Celo, V., Brook, J. R., Mathieu, D., Ding, L., and Austin, C. C.: Canadian National Air Pollution Surveillance (NAPS) $PM_{2.5}$ speciation program: Methodology and $PM_{2.5}$ chemical composition for the years 2003–2008, Atmos. Environ., 45, 673-686, doi: 10.1016/j.atmosenv.2010.10.024, 2011.

Dall'Osto, M., Querol, X., Amato, F., Karanasiou, A., Lucarelli, F., Nava, S., Calzolai, G., and Chiari, M.: Hourly elemental concentrations in $PM_{2.5}$ aerosols sampled simultaneously at urban background and road site during SAPUSS - diurnal variations and PMF receptor modelling, Atmos. Chem. Phys., 13, 4375-4392, doi: 10.5194/acp-13-4375-2013, 2013.

DeCarlo, P. F., Kimmel, J. R., Trimborn, A., Northway, M. J., Jayne, J. T., Aiken, A. C., Gonin, M., Fuhrer, K., Horvath, T., Docherty, K. S., Worsnop, D. R., and Jimenez,

J. L.: Field-deployable, high-resolution, time-of-flight aerosol mass spectrometer, Anal. Chem., 78, 8281-8289, doi: 10.1021/ac061249n, 2006.

Duan, J. and Tan, J.: Atmospheric heavy metals and arsenic in China: Situation, sources and control policies, Atmos. Environ., 74, 93-101, doi: 10.1016/j.atmosenv.2013.03.031, 2013.

Duffus John, H.: "Heavy metals"-a meaningless term?, Pure Appl. Chem., 74, 793-807, doi: 10.1351/pac200274050793, 2002.

Fan, Q., Zhang, Y., Ma, W., Ma, H., Feng, J., Yu, Q., Yang, X., Ng, S. K. W., Fu, Q., and Chen, L.: Spatial and seasonal dynamics of ship emissions over the Yangtze River Delta and East China Sea and their potential environmental influence, Environ. Sci. Technol., 50, 1322-1329, doi: 10.1021/acs.est.5b03965, 2016.

Fang, T., Guo, H., Verma, V., Peltier, R. E., and Weber, R. J.: $PM_{2.5}$ water-soluble elements in the southeastern United States: Automated analytical method development, spatiotemporal distributions, source apportionment, and implications for heath studies, Atmos. Chem. Phys., 15, 11667-11682, doi: 10.5194/acp-15-11667-2015, 2015.

Fergusson, J. E.: The heavy elements: Chemistry, environmental impact and health effects, Pergamon Press, Oxford, UK, pp 614, 1990.

Friendly, M.: Corrgrams: Exploratory displays for correlation matrices, Am. Stat., 56, 316-324, doi: 10.1198/000313002533, 2002.

Geagea, M. L., Stille, P., Millet, M., and Perrone, T.: REE characteristics and Pb, Sr and Nd isotopic compositions of steel plant emissions, Sci. Total Environ., 373, 404-419, doi: 10.1016/j.scitotenv.2006.11.011, 2007.

Gross, D. S., Gälli, M. E., Silva, P. J., and Prather, K. A.: Relative sensitivity factors for alkali metal and ammonium cations in single-particle aerosol time-of-flight mass spectra, Anal. Chem., 72, 416-422, doi: 10.1021/ac990434g, 2000.

Han, T., Qiao, L., Zhou, M., Qu, Y., Du, J., Liu, X., Lou, S., Chen, C., Wang, H., Zhang, F., Yu, Q., and Wu, Q.: Chemical and optical properties of aerosols and their interrelationship in winter in the megacity Shanghai of China, J. Environ. Sci. (China), 27, 59-69, doi: 10.1016/j.jes.2014.04.018, 2015.

Harrison, R. M., Jones, A. M., Gietl, J., Yin, J., and Green, D. C.: Estimation of the contributions of brake dust, tire wear, and resuspension to nonexhaust traffic particles derived from atmospheric measurements, Environ. Sci. Technol., 46, 6523-6529, doi: 10.1021/es300894r, 2012.

Heo, J. B., Hopke, P. K., and Yi, S. M.: Source apportionment of $PM_{2.5}$ in Seoul, Korea, Atmos. Chem. Phys., 9, 4957-4971, doi: 10.5194/acp-9-4957-2009, 2009.

Holden, P. A., Gardea-Torresdey, J. L., Klaessig, F., Turco, R. F., Mortimer, M., Hund-Rinke, K., Cohen Hubal, E. A., Avery, D., Barceló, D., Behra, R., Cohen, Y., Deydier-Stephan, L., Ferguson, P. L., Fernandes, T. F., Herr Harthorn, B., Henderson, W. M., Hoke, R. A., Hristozov, D., Johnston, J. M., Kane, A. B., Kapustka, L., Keller, A. A., Lenihan, H. S., Lovell, W., Murphy, C. J., Nisbet, R. M., Petersen, E. J., Salinas, E. R., Scheringer, M., Sharma, M., Speed, D. E., Sultan, Y., Westerhoff, P., White, J. C., Wiesner, M. R., Wong, E. M., Xing, B., Steele Horan, M., Godwin, H. A., and Nel, A. E.: Considerations of environmentally

relevant test conditions for improved evaluation of ecological hazards of engineered nanomaterials, Environ. Sci. Technol., 50, 6124-6145, doi: 10.1021/acs.est.6b00608, 2016.

Honda, T., Eliot, M. N., Eaton, C. B., Whitsel, E., Stewart, J. D., Mu, L., Suh, H., Szpiro, A., Kaufman, J. D., Vedal, S., and Wellenius, G. A.: Long-term exposure to residential ambient fine and coarse particulate matter and incident hypertension in post-menopausal women, Environ. Int., 105, 79-85, doi: 10.1016/j.envint.2017.05.009, 2017.

Hu, X., Zhang, Y., Ding, Z., Wang, T., Lian, H., Sun, Y., and Wu, J.: Bioaccessibility and health risk of arsenic and heavy metals (Cd, Co, Cr, Cu, Ni, Pb, Zn and Mn) in TSP and $PM_{2.5}$ in Nanjing, China, Atmos. Environ., 57, 146-152, doi: 10.1016/j.atmosenv.2012.04.056, 2012.

Huang, C., Chen, C. H., Li, L., Cheng, Z., Wang, H. L., Huang, H. Y., Streets, D. G., Wang, Y. J., Zhang, G. F., and Chen, Y. R.: Emission inventory of anthropogenic air pollutants and VOC species in the Yangtze River Delta region, China, Atmos. Chem. Phys., 11, 4105-4120, DOI 10.5194/acp-11-4105-2011, 2011.

Huang, K., Zhuang, G., Lin, Y., Wang, Q., Fu, J. S., Fu, Q., Liu, T., and Deng, C.: How to improve the air quality over megacities in China: Pollution characterization and source analysis in Shanghai before, during, and after the 2010 World Expo, Atmos. Chem. Phys., 13, 5927-5942, doi: 10.5194/acp-13-5927-2013, 2013.

Huang, W., Cao, J., Tao, Y., Dai, L., Lu, S.-E., Hou, B., Wang, Z., and Zhu, T.: Seasonal variation of chemical species associated with short-term mortality effects of $PM_{2.5}$ in Xi'an, a central city in China, Am. J. Epidemiol., 175, 556-566, doi: 10.1093/aje/kwr342, 2012.

Iyengar, V. and Woittiez, J.: Trace elements in human clinical specimens: evaluation of literature data to identify reference values, Clin. Chem., 34, 474-481, 1988.

Jeong, C. H., Wang, J. M., and Evans, G. J.: Source apportionment of urban particulate matter using hourly resolved trace metals, organics, and inorganic aerosol components, Atmos. Chem. Phys. Discuss., 1-32, doi: 10.5194/acp-2016-189, 2016.

Jomova, K. and Valko, M.: Advances in metal-induced oxidative stress and human disease, Toxicol., 283, 65-87, doi: 10.1016/j.tox.2011.03.001, 2011.

Kastury, F., Smith, E., and Juhasz, A. L.: A critical review of approaches and limitations of inhalation bioavailability and bioaccessibility of metal(loid)s from ambient particulate matter or dust, Sci. Total Environ., 574, 1054-1074, doi: 10.1016/j.scitotenv.2016.09.056, 2017.

Kim, K. H., Kabir, E., and Jahan, S. A.: A review on the distribution of Hg in the environment and its human health impacts, J. Hazard. Mater., 306, 376-385, doi: 10.1016/j.jhazmat.2015.11.031, 2016.

Kloog, I., Ridgway, B., Koutrakis, P., Coull, B. A., and Schwartz, J. D.: Long- and short-term exposure to $PM_{2.5}$ and mortality: Using novel exposure models, Epidemiol., 24, 555-561, doi: 10.1097/EDE.0b013e318294beaa, 2013.

Leung, A. O. W., Duzgoren-Aydin, N. S., Cheung, K. C., and Wong, M. H.: Heavy metals concentrations of surface dust from e-waste recycling and its human health

implications in Southeast China, Environ. Sci. Technol., 42, 2674-2680, doi: 10.1021/es071873x, 2008.

Li, H., Wang, J., Wang, Q., Tian, C., Qian, X., and Leng, X.: Magnetic properties as a proxy for predicting fine-particle-bound heavy metals in a support vector machine approach, Environ. Sci. Technol., Just accepted, doi: 10.1021/acs.est.7b00729, 2017.

Litter, M. I.: Heterogeneous photocatalysis: Transition metal ions in photocatalytic systems, Appl. Catal. B: Environ., 23, 89-114, doi: 10.1016/S0926-3373(99)00069-7, 1999.

Liu, Z., Hu, B., Wang, L., Wu, F., Gao, W., and Wang, Y.: Seasonal and diurnal variation in particulate matter (PM_{10} and $PM_{2.5}$) at an urban site of Beijing: Analyses from a 9-year study, Environ. Sci. Pollut. Res. Int., 22, 627-642, doi: 10.1007/s11356-014-3347-0, 2015.

Liu, Z., Lu, X., Feng, J., Fan, Q., Zhang, Y., and Yang, X.: Influence of ship emissions on urban air quality: A comprehensive study using highly time-resolved online measurements and numerical simulation in Shanghai, Environ. Sci. Technol., 51, 202-211, doi: 10.1021/acs.est.6b03834, 2017.

Lu, S., Yao, Z., Chen, X., Wu, M., Sheng, G., Fu, J., and Paul, D.: The relationship between physicochemical characterization and the potential toxicity of fine particulates ($PM_{2.5}$) in Shanghai atmosphere, Atmos. Environ., 42, 7205-7214, doi: 10.1016/j.atmosenv.2008.07.030, 2008.

Maenhaut, W.: Present role of PIXE in atmospheric aerosol research, Nucl. Instrum. Meth. B, 363, 86-91, doi: 10.1016/j.nimb.2015.07.043, 2015.

Morman, S. A. and Plumlee, G. S.: The role of airborne mineral dusts in human disease, Aeolian Res., 9, 203-212, doi: 10.1016/j.aeolia.2012.12.001, 2013.

Murdoch, D. J. and Chow, E. D.: A graphical display of large correlation matrices, Am. Stat., 50, 178-180, doi: 10.1080/00031305.1996.10474371, 1996.

Murphy, D. M., Thomson, D. S., and Mahoney, M. J.: In situ measurements of organics, meteoritic material, mercury, and other elements in aerosols at 5 to 19 kilometers, Science, 282, 1664-1669, doi: 10.1126/science.282.5394.1664, 1998.

Normile, D.: China's living laboratory in urbanization, Science, 319, 740-743, doi: 10.1126/science.319.5864.740, 2008.

Nriagu, J. O.: A history of global metal pollution, Science, 272, 223-223, doi: 10.1126/science.272.5259.223, 1996.

Olujimi, O. O., Oputu, O., Fatoki, O., Opatoyinbo, O. E., Aroyewun, O. A., and Baruani, J.: Heavy metals speciation and human health risk assessment at an illegal gold mining site in Igun, Osun State, Nigeria, J. Heal. Pollut., 5, 19-32, doi: 10.5696/i2156-9614-5-8.19, 2015.

Pardo, M., Shafer, M. M., Rudich, A., Schauer, J. J., and Rudich, Y.: Single exposure to near roadway particulate matter leads to confined inflammatory and defense responses: Possible role of metals, Environ. Sci. Technol., 49, 8777-8785, doi: 10.1021/acs.est.5b01449, 2015.

Park, S. S., Cho, S. Y., Jo, M. R., Gong, B. J., Park, J. S., and Lee, S. J.: Field evaluation of a near-real time elemental monitor and identification of element sources

observed at an air monitoring supersite in Korea, Atmos. Pollut. Res., 5, 119-128, doi: 10.5094/apr.2014.015, 2014.

Phillips-Smith, C., Jeong, C. H., Healy, R. M., Dabek-Zlotorzynska, E., Celo, V., Brook, J. R., and Evans, G.: Sources of particulate matter in the Athabasca oil sands region: Investigation through a comparison of trace element measurement methodologies, Atmos. Chem. Phys. Discuss., 2017, 1-34, doi: 10.5194/acp-2016-966, 2017.

Pope III, C. A., Burnett, R. T., Thun, M. J., Calle, E. E., Krewski, D., Ito, K., and Thurston, G. D.: Lung cancer, cardiopulmonary mortality, and long-term exposure to fine particulate air pollution, J. Am. Med. Assoc., 1132-1141, 2002.

Pope III, C. A., Ezzati, M., and Dockery, D. W.: Fine-particulate air pollution and life expectancy in the United States, New Engl. J. Med., 360, 376-386, doi: 10.1056/NEJMsa0805646, 2009.

Qiao, L., Cai, J., Wang, H., Wang, W., Zhou, M., Lou, S., Chen, R., Dai, H., Chen, C., and Kan, H.: $PM_{2.5}$ constituents and hospital emergency-room visits in Shanghai, China, Environ. Sci. Technol., 48, 10406-10414, doi: 10.1021/es501305k, 2014.

Reff, A., Bhave, P. V., Simon, H., Pace, T. G., Pouliot, G. A., Mobley, J. D., and Houyoux, M.: Emissions Inventory of $PM_{2.5}$ trace elements across the United States, Environ. Sci. Technol., 43, 5790-5796, doi: 10.1021/es802930x, 2009.

Ren, D. Y.: Geochemistry of trace elements in coal, Science Press, Beijing, 2006. (In Chinese)

Richard, A., Bukowiecki, N., Lienemann, P., Furger, M., Fierz, M., Minguillón, M. C., Weideli, B., Figi, R., Flechsig, U., Appel, K., Prévôt, A. S. H., and Baltensperger, U.: Quantitative sampling and analysis of trace elements in atmospheric aerosols: impactor characterization and Synchrotron-XRF mass calibration, Atmos. Meas. Tech., 3, 1473-1485, doi: 10.5194/amt-3-1473-2010, 2010.

Ridley, D. A., Heald, C. L., Kok, J. F., and Zhao, C.: An observationally constrained estimate of global dust aerosol optical depth, Atmos. Chem. Phys., 16, 15097-15117, doi: 10.5194/acp-16-15097-2016, 2016.

Rubasinghege, G., Elzey, S., Baltrusaitis, J., Jayaweera, P. M., and Grassian, V. H.: Reactions on atmospheric dust particles: Surface photochemistry and size-dependent nanoscale redox chemistry, J. Phys. Chem. Let., 1, 1729-1737, doi: 10.1021/jz100371d, 2010a.

Rubasinghege, G., Lentz, R. W., Scherer, M. M., and Grassian, V. H.: Simulated atmospheric processing of iron oxyhydroxide minerals at low pH: Roles of particle size and acid anion in iron dissolution, P. Natl. Acad. Sci., 107, 6628-6633, doi: 10.1073/pnas.0910809107, 2010b.

Saffari, A., Daher, N., Shafer, M. M., Schauer, J. J., and Sioutas, C.: Global perspective on the oxidative potential of airborne particulate matter: A synthesis of research findings, Environ. Sci. Technol., 48, 7576-7583, doi: 10.1021/es500937x, 2014.

Schlosser, E., Fernholz, T., Teichert, H., and Ebert, V.: In situ detection of potassium atoms in high-temperature coal-combustion systems using near-infrared-diode lasers, Spectrochim. Acta A, 58, 2347-2359, doi: 10.1016/S1386-1425(02)00049-5, 2002.

Seigneur, C. and Constantinou, E.: Chemical kinetic mechanism for atmospheric

chromium, Environ. Sci. Technol., 29, 222-231, doi: 10.1021/es00001a029, 1995.

Shah, A. S. V., Langrish, J. P., Nair, H., McAllister, D. A., Hunter, A. L., Donaldson, K., Newby, D. E., and Mills, N. L.: Global association of air pollution and heart failure: A systematic review and meta-analysis, Lancet, 382, 1039-1048, doi: 10.1016/s0140-6736(13)60898-3, 2013.

Shu, J., Dearing, J. A., Morse, A. P., Yu, L., and Yuan, N.: Determining the sources of atmospheric particles in Shanghai, China, from magnetic and geochemical properties, Atmos. Environ., 35, 2615-2625, doi: 10.1016/S1352-2310(00)00454-4, 2001.

Sofowote, U. M., Su, Y., Dabek-Zlotorzynska, E., Rastogi, A. K., Brook, J., and Hopke, P. K.: Sources and temporal variations of constrained PMF factors obtained from multiple-year receptor modeling of ambient $PM_{2.5}$ data from five speciation sites in Ontario, Canada, Atmos. Environ., 108, 140-150, doi: 10.1016/j.atmosenv.2015.02.055, 2015.

Strak, M., Janssen, N. A., Godri, K. J., Gosens, I., Mudway, I. S., Cassee, F. R., Lebret, E., Kelly, F. J., Harrison, R. M., Brunekreef, B., Steenhof, M., and Hoek, G.: Respiratory health effects of airborne particulate matter: The role of particle size, composition, and oxidative potential-the RAPTES project, Environ. Health. Perspect., 120, 1183-1189, doi: 10.1289/ehp.1104389, 2012.

Streit, B.: Lexikon der Ökotoxikologie, Wiley-VCH, Weinheim, Germany, 1991.

Strickland, M. J., Hao, H., Hu, X., Chang, H. H., Darrow, L. A., and Liu, Y.: Pediatric emergency visits and short-term changes in $PM_{2.5}$ concentrations in the U.S. State of Georgia, Environ. Health. Perspect., 124, 690-696, doi: 10.1289/ehp.1509856, 2016.

Tang, M., Huang, X., Lu, K., Ge, M., Li, Y., Cheng, P., Zhu, T., Ding, A., Zhang, Y., Gligorovski, S., Song, W., Ding, X., Bi, X., and Wang, X.: Heterogeneous reactions of mineral dust aerosol: Implications for tropospheric oxidation capacity, Atmos. Chem. Phys. Discuss., 2017, 1-124, doi: 10.5194/acp-2017-458, 2017.

Tchounwou, P. B., Yedjou, C. G., Patlolla, A. K., and Sutton, D. J.: Heavy metals toxicity and the environment. In Molecular, Clinical and Environmental Toxicology, 133-164, ISBN: 978-3-7643-8337-4, 2012.

Thompson, D., and Argent, B. B.: The mobilisation of sodium and potassium during coal combustion and gasification, Fuel, 78, 1679-1689, doi: 10.1016/S0016-2361(99)00115-5, 1999.

Thorpe, A., and Harrison, R. M.: Sources and properties of non-exhaust particulate matter from road traffic: A review, Sci. Total Environ., 400, 270-282, doi: 10.1016/j.scitotenv.2008.06.007, 2008.

Tian, H. Z., Zhu, C. Y., Gao, J. J., Cheng, K., Hao, J. M., Wang, K., Hua, S. B., Wang, Y., and Zhou, J. R.: Quantitative assessment of atmospheric emissions of toxic heavy metals from anthropogenic sources in China: Historical trend, spatial distribution, uncertainties, and control policies, Atmos. Chem. Phys., 15, 10127-10147, doi: 10.5194/acp-15-10127-2015, 2015.

Traversi, R., Becagli, S., Calzolai, G., Chiari, M., Giannoni, M., Lucarelli, F., Nava, S., Rugi, F., Severi, M., and Udisti, R.: A comparison between PIXE and ICP-AES

measurements of metals in aerosol particulate collected in urban and marine sites in Italy, Nucl. Instrum. Meth. B, 318, 130-134, doi: 10.1016/j.nimb.2013.05.102, 2014.

Usher, C. R., Michel, A. E., and Grassian, V. H.: Reactions on mineral dust, Chem. Rev., 103, 4883-4940, doi: 10.1021/cr020657y, 2003.

Venter, A. D., van Zyl, P. G., Beukes, J. P., Josipovic, M., Hendriks, J., Vakkari, V., and Laakso, L.: Atmospheric trace metals measured at a regional background site (Welgegund) in South Africa, Atmos. Chem. Phys., 17, 4251-4263, doi: 10.5194/acp-17-4251-2017, 2017.

Verma, V., Shafer, M. M., Schauer, J. J., and Sioutas, C.: Contribution of transition metals in the reactive oxygen species activity of PM emissions from retrofitted heavy-duty vehicles, Atmos. Environ., 44, 5165-5173, doi: 10.1016/j.atmosenv.2010.08.052, 2010.

Visser, S., Slowik, J. G., Furger, M., Zotter, P., Bukowiecki, N., Canonaco, F., Flechsig, U., Appel, K., Green, D. C., Tremper, A. H., Young, D. E., Williams, P. I., Allan, J. D., Coe, H., Williams, L. R., Mohr, C., Xu, L., Ng, N. L., Nemitz, E., Barlow, J. F., Halios, C. H., Fleming, Z. L., Baltensperger, U., and Prévôt, A. S. H.: Advanced source apportionment of size-resolved trace elements at multiple sites in London during winter, Atmos. Chem. Phys., 15, 11291-11309, doi: 10.5194/acp-15-11291-2015, 2015a.

Visser, S., Slowik, J. G., Furger, M., Zotter, P., Bukowiecki, N., Dressler, R., Flechsig, U., Appel, K., Green, D. C., Tremper, A. H., Young, D. E., Williams, P. I., Allan, J. D., Herndon, S. C., Williams, L. R., Mohr, C., Xu, L., Ng, N. L., Detournay, A., Barlow, J. F., Halios, C. H., Fleming, Z. L., Baltensperger, U., and Prévôt, A. S. H.: Kerb and urban increment of highly time-resolved trace elements in PM_{10}, $PM_{2.5}$ and PM_{10} winter aerosol in London during ClearfLo 2012, Atmos. Chem. Phys., 15, 2367-2386, doi: 10.5194/acp-15-2367-2015, 2015b.

Wang, F., Chen, Y., Meng, X., Fu, J., and Wang, B.: The contribution of anthropogenic sources to the aerosols over East China Sea, Atmos. Environ., 127, 22-33, doi: 10.1016/j.atmosenv.2015.12.002, 2016.

Wang, J., Hu, Z., Chen, Y., Chen, Z., and Xu, S.: Contamination characteristics and possible sources of PM_{10} and $PM_{2.5}$ in different functional areas of Shanghai, China, Atmos. Environ., 68, 221-229, doi: 10.1016/j.atmosenv.2012.10.070, 2013.

Wang, X., Bi, X., Sheng, G., and Fu, J.: Hospital indoor $PM_{10}/PM_{2.5}$ and associated trace elements in Guangzhou, China, Sci. Total Environ., 366, 124-135, doi: 10.1016/j.scitotenv.2005.09.004, 2006.

Wei, T. and Simko, V.: Corrplot: Visualization of a correlation matrix. R package version 0.77, available online at http://cran.r-project.org/package=corrplot, 2016. (last accessible: 7/7/2017)

West, J. J., Cohen, A., Dentener, F., Brunekreef, B., Zhu, T., Armstrong, B., Bell, M. L., Brauer, M., Carmichael, G., Costa, D. L., Dockery, D. W., Kleeman, M., Krzyzanowski, M., Kunzli, N., Liousse, C., Lung, S. C., Martin, R. V., Poschl, U., Pope, C. A., 3rd, Roberts, J. M., Russell, A. G., and Wiedinmyer, C.: "What we breathe impacts our health: Improving understanding of the link between air

pollution and health", Environ. Sci. Technol., 50, 4895-4904, doi: 10.1021/acs.est.5b03827, 2016.

Westberg, H. M., Byström, M., and Leckner, B.: Distribution of potassium, chlorine, and sulfur between solid and vapor phases during combustion of wood chips and coal, Energy Fuel., 17, 18-28, doi: 10.1021/ef020060l, 2003.

WHO (World Health Organization) Air quality guidelines - global update 2005, available online at http://www.who.int/phe/health_topics/outdoorair/outdoorair_aqg/en/, 2005. (last accessible: 7/7/2017)

Xie, S. D., Liu, Z., Chen, T., and Hua, L.: Spatiotemporal variations of ambient PM_{10} source contributions in Beijing in 2004 using positive matrix factorization, Atmos. Chem. Phys., 8, 2701-2716, doi: 10.5194/acp-8-2701-2008, 2008.

Yanca, C. A., Barth, D. C., Petterson, K. A., Nakanishi, M. P., Cooper, J. A., Johnsen, B. E., Lambert, R. H., and Bivins, D. G.: Validation of three new methods for determination of metal emissions using a modified Environmental Protection Agency Method 301, J. Air Waste Manage. Assoc., 56, 1733-1742, doi: 10.1080/10473289.2006.10464578, 2006.

Zhang, X. K.: The content of trace metals in coals from Shanxi, Henan Province and their mode of occurrences. Henan Polytechnic University, Master's Dissertation, 2010 (In Chinese with English abstract).

Zhao, J., Lewinski, N., and Riediker, M.: Physico-chemical characterization and oxidative reactivity evaluation of aged brake wear particles, Aerosol Sci. Technol., 49, 65-74, doi: 10.1080/02786826.2014.998363, 2015.

Zheng, J., Tan, M., Shibata, Y., Tanaka, A., Li, Y., Zhang, G., Zhang, Y., and Shan, Z.: Characteristics of lead isotope ratios and elemental concentrations in PM_{10} fraction of airborne particulate matter in Shanghai after the phase-out of leaded gasoline, Atmos. Environ., 38, 1191-1200, doi: 10.1016/j.atmosenv.2003.11.004, 2004.

Atmos. Chem. Phys. Discuss., https://doi.org/10.5194/acp-2017-613
Manuscript under review for journal Atmos. Chem. Phys.
Discussion started: 1 August 2017

Atmospheric Chemistry and Physics Discussions

Table 1. A collection of long-term and high-time resolution measurements of ambient trace elements concentrations (ng m^{-3}) in fine particles.

Species	Shanghai, CN[a]	Wood Buffalo, CA[b]	Gwangju, KP[c]	London, UK[d]	London, UK[e]	Barcelona, ES[f]	Toronto, CA[g]
Ag	3.9	/	/	/	/	/	/
As	6.6	/	9.6	/	/	/	/
Au	2.2	/	/	/	/	/	/
Ba	24.2	/	52.0	10.3	3.7	/	1.9
Ca	191.5	54.0	122	78.7	50.1	130.0	54.0
Cd	9.6	/	/	/	/	/	/
Cr	4.5	0.04	/	2.3	0.8	8.0	0.24
Cu	12.0	2.04	15.5	12.8	4.9	8.0	3.1
Fe	406.2	60.0	293.0	350.3	118.9	131.0	76.8
Hg	2.2	/	/	/	/	/	/
K	388.6	31.0	732.0	27.2	23.7	82.0	27.1
Mn	31.7	1.12	24.0	4.8	2.5	6.0	1.8
Ni	6.0	0.08	3.8	0.5	0.2	3.0	0.21
Pb	27.2	/	49.0	2.3	1.8	12.0	2.4
Se	2.6	/	4.3	/	/	/	0.3
Si	638.7	143	/	/	/	/	/
V	13.4	0.21	4.6	1.3	0.6	8.0	0.11
Zn	120.3	0.88	103.0	8.9	5.3	25.0	11.3

Note: a, this study; b, Phillips-Smith et al., 2017; c, Park et al., 2014; d, $PM_{0.3\text{-}2.5}$, Marylebone Road (Visser et al., 2015b); e, $PM_{0.3\text{-}2.5}$, North Kensington (Visser et al., 2015b); f, Road site (Dall'Osto et al., 2013); g, Sofowote et al., 2015. We noticed that although a huge data set of hourly resolved trace metals had been reported in Jeong et al. (2016) and Visser et al. (2015a), in which no detailed information regarding the specific mass concentrations of trace metals were given.

Atmos. Chem. Phys. Discuss., https://doi.org/10.5194/acp-2017-613
Manuscript under review for journal Atmos. Chem. Phys.
Discussion started: 1 August 2017

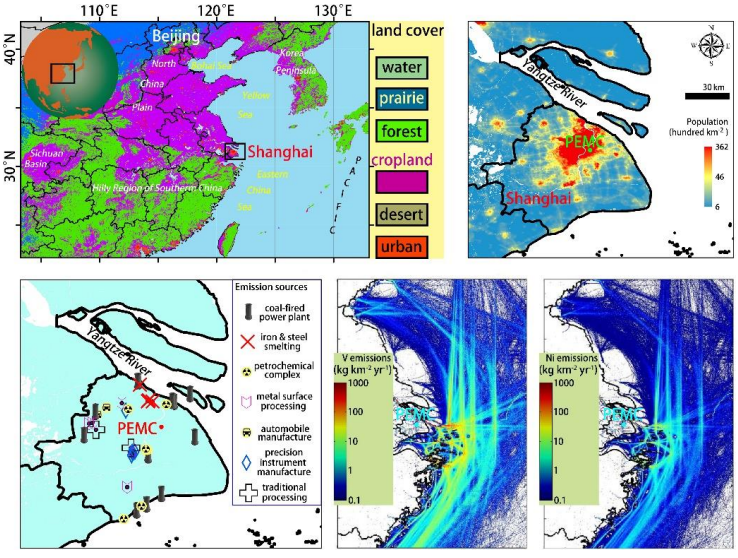

1015 **Figure 1.** A land uses map indicating the location of Shanghai (**a**; black box), as well as the population density (**b**) and the major point sources (**c**) around the sampling site (PEMC). The emissions of V (**d**) and Ni (**e**) from shipping in the YRD and the East China Sea within 400 km of the coastline were estimated based on an automatic identification system model (adopted from (Fan et al., 2016)).

1020

Atmos. Chem. Phys. Discuss., https://doi.org/10.5194/acp-2017-613
Manuscript under review for journal Atmos. Chem. Phys.
Discussion started: 1 August 2017

Atmospheric Chemistry and Physics Discussions

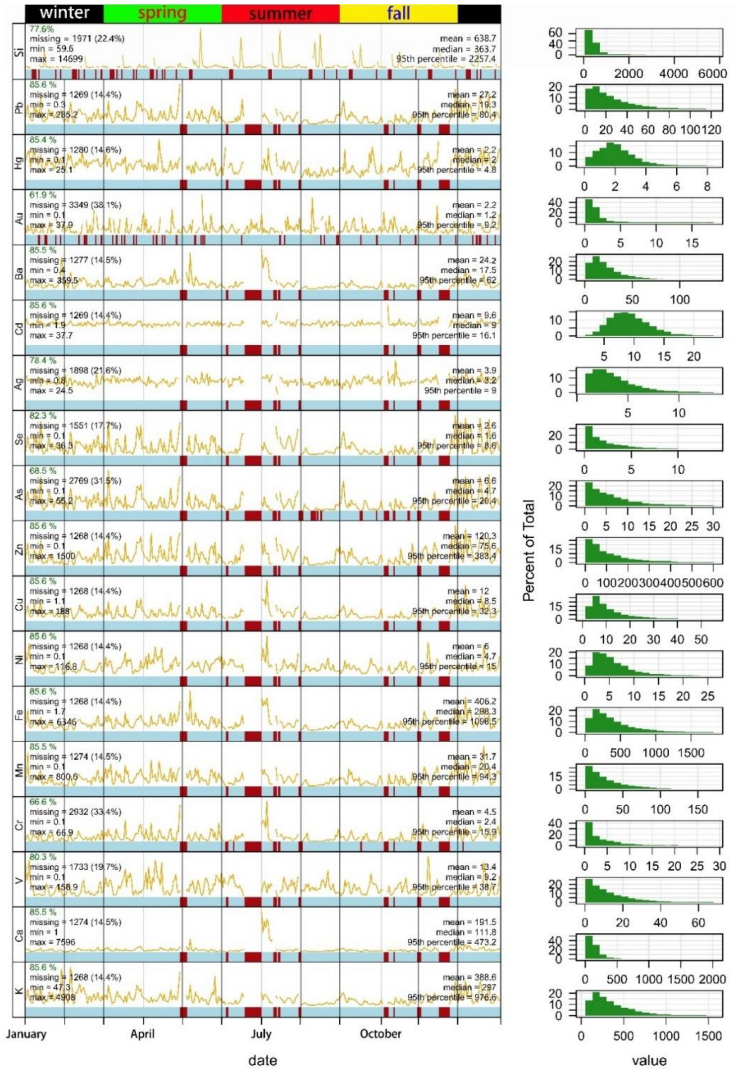

Figure 2. General statistical summaries of 18 trace elements measured in Shanghai. The plots in the left panel show the time series data, where blue shows the presence of data and red shows missing data. The mean daily values are also shown in pale yellow scaled to cover the range in the data from zero to the maximum daily value. As such, the daily values are indicative of an overall trend rather than conveying quantitative information. For each elemental species, the overall summary statistics are given. The panels on the right show the distribution of each elemental species using a histogram plot.

Atmos. Chem. Phys. Discuss., https://doi.org/10.5194/acp-2017-613
Manuscript under review for journal Atmos. Chem. Phys.
Discussion started: 1 August 2017

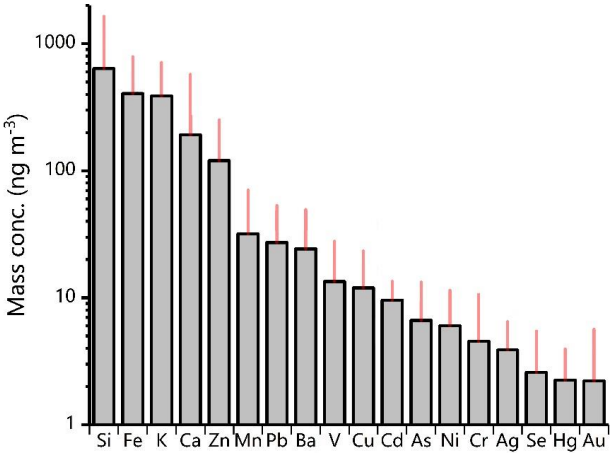

Figure 3. A quick glance of the mass concentrations of 18 trace elements measured in Shanghai as sorted from high to low (log10 scaling). The dark red line indicates one standard deviation.

Atmos. Chem. Phys. Discuss., https://doi.org/10.5194/acp-2017-613
Manuscript under review for journal Atmos. Chem. Phys.
Discussion started: 1 August 2017

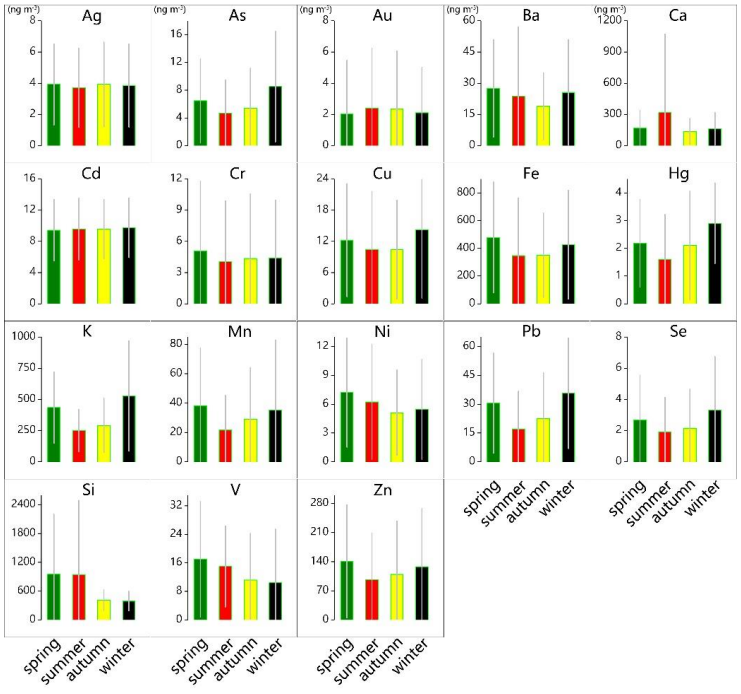

Figure 4. Seasonal variations of mass concentrations for 18 trace elements measured in Shanghai between March 2016 and February 2017. The gray line indicates one two standard deviations. Four seasons in Shanghai were defined as follows: March-May as spring, June-August as summer, September- November as fall, and December and January-February as winter.

Atmos. Chem. Phys. Discuss., https://doi.org/10.5194/acp-2017-613
Manuscript under review for journal Atmos. Chem. Phys.
Discussion started: 1 August 2017

Atmospheric Chemistry and Physics Discussions

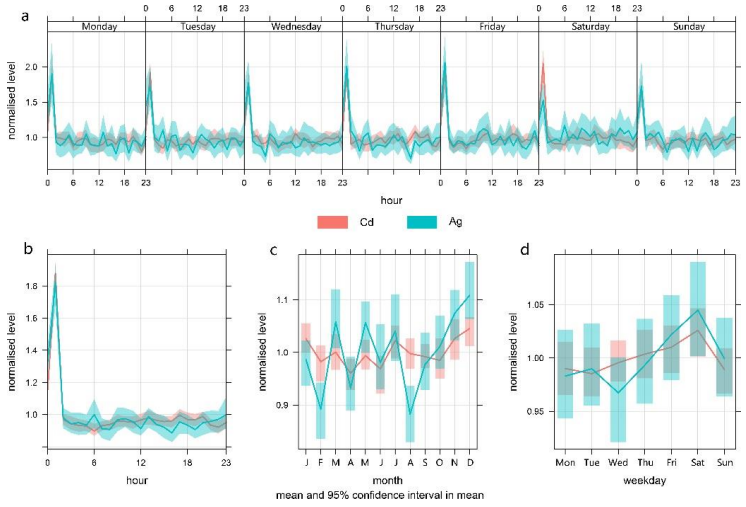

Figure 5. Weekly diurnal (**a**), diurnal (**b**), monthly (**c**), and weekly (**d**) variations of normalized Cd and Ag concentrations in Shanghai.

Atmos. Chem. Phys. Discuss., https://doi.org/10.5194/acp-2017-613
Manuscript under review for journal Atmos. Chem. Phys.
Discussion started: 1 August 2017

Atmospheric Chemistry and Physics Discussions

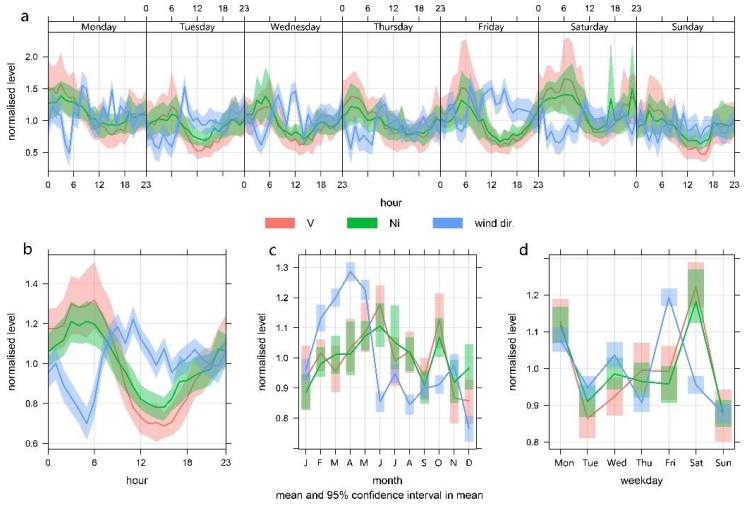

Figure 6. Weekly diurnal (**a**), diurnal (**b**), monthly (**c**), and weekly (**d**) variations of normalized V and Ni concentrations, and wind directions in Shanghai.

Atmos. Chem. Phys. Discuss., https://doi.org/10.5194/acp-2017-613
Manuscript under review for journal Atmos. Chem. Phys.
Discussion started: 1 August 2017

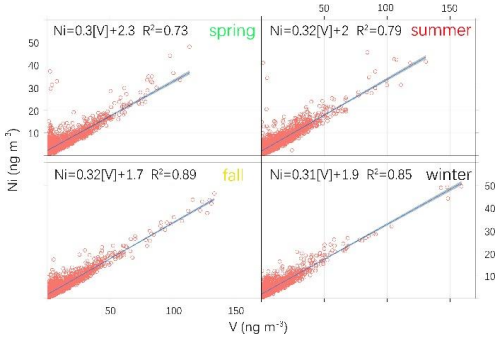

Figure 7. Linear correlation analysis between V (x axis) and Ni (y axis) in Shanghai during four seasons.

Atmos. Chem. Phys. Discuss., https://doi.org/10.5194/acp-2017-613
Manuscript under review for journal Atmos. Chem. Phys.
Discussion started: 1 August 2017

Atmospheric Chemistry and Physics Discussions

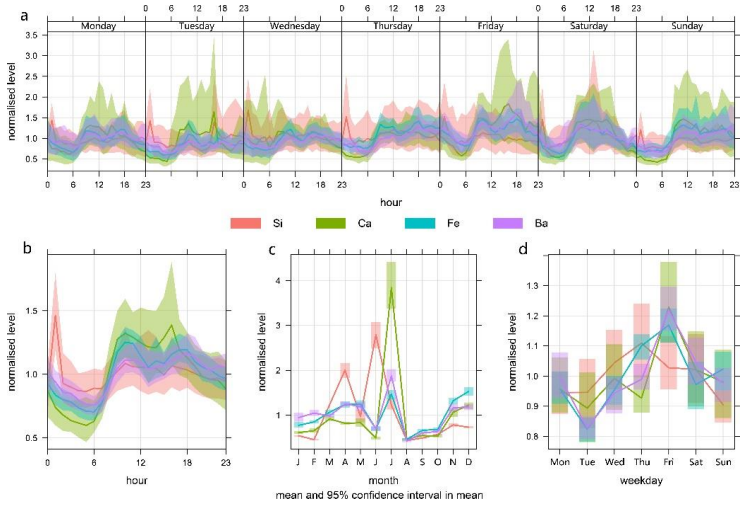

Figure 8. Weekly diurnal (**a**), diurnal (**b**), monthly (**c**), and weekly (**d**) variations of normalized Si, Ca, Fe, and Ba concentrations in Shanghai.

Atmos. Chem. Phys. Discuss., https://doi.org/10.5194/acp-2017-613
Manuscript under review for journal Atmos. Chem. Phys.
Discussion started: 1 August 2017

Atmospheric Chemistry and Physics Discussions

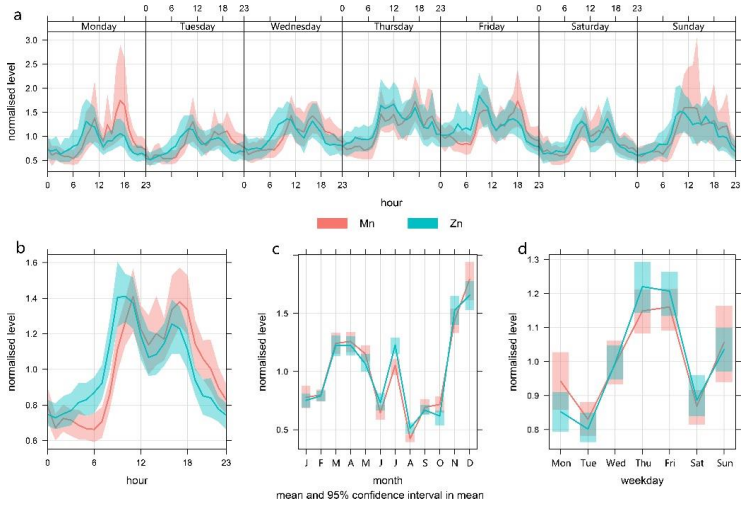

Figure 9. Weekly diurnal (**a**), diurnal (**b**), monthly (**c**), and weekly (**d**) variations of normalized Mn and Zn concentrations in Shanghai.

Atmos. Chem. Phys. Discuss., https://doi.org/10.5194/acp-2017-613
Manuscript under review for journal Atmos. Chem. Phys.
Discussion started: 1 August 2017

Atmospheric Chemistry and Physics Discussions

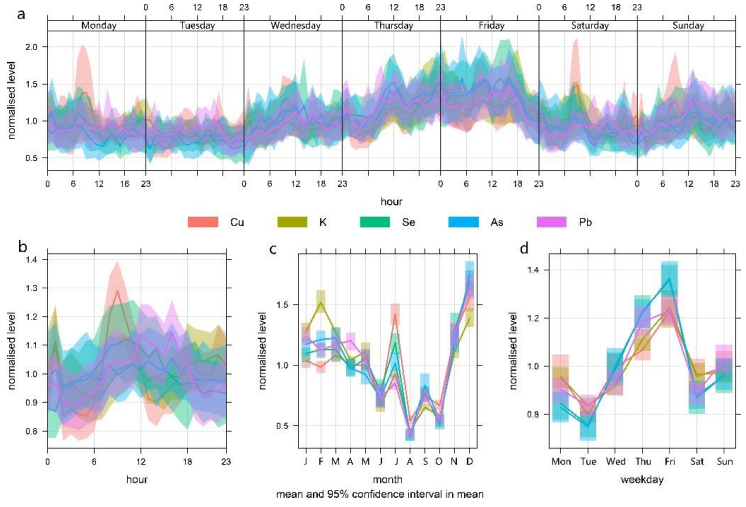

Figure 10. Weekly diurnal (**a**), diurnal (**b**), monthly (**c**), and weekly (**d**) variations of normalized Cu, K, Se, As, and Pb concentrations in Shanghai.

Atmos. Chem. Phys. Discuss., https://doi.org/10.5194/acp-2017-613
Manuscript under review for journal Atmos. Chem. Phys.
Discussion started: 1 August 2017

Atmospheric Chemistry and Physics Discussions

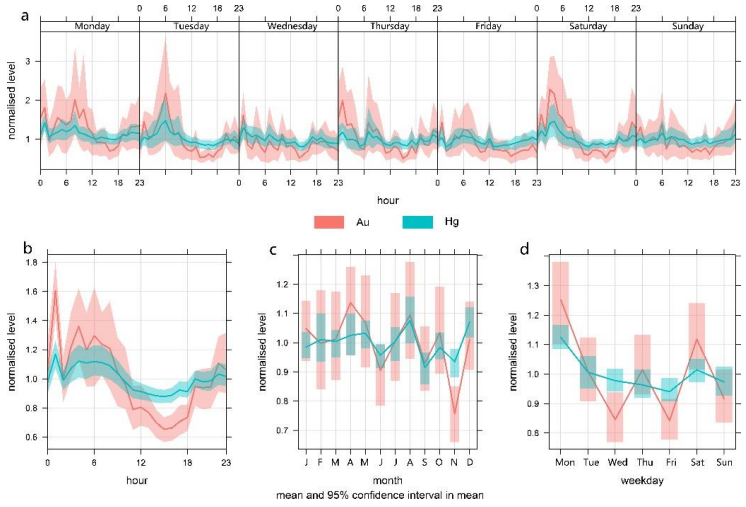

Figure 11. Weekly diurnal (**a**), diurnal (**b**), monthly (**c**), and weekly (**d**) variations of normalized Au and Hg concentrations in Shanghai.

Atmos. Chem. Phys. Discuss., https://doi.org/10.5194/acp-2017-613
Manuscript under review for journal Atmos. Chem. Phys.
Discussion started: 1 August 2017

Atmospheric Chemistry and Physics Discussions

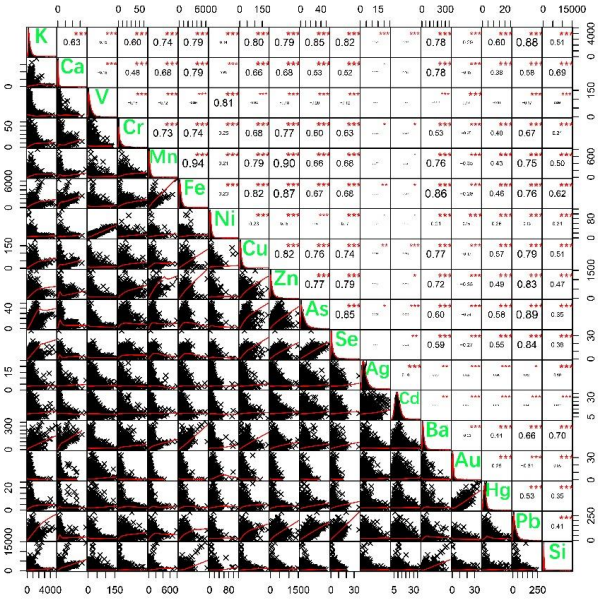

Figure 12. Spearman correlation matrix of 18 atmospheric elemental species in Shanghai between March 2016 and February 2017. The distribution of each species is shown on the diagonal. On the bottom of the diagonal, the bivariate scatter plots with a fitted line are displayed; on the top of the diagonal, the value of the correlation plus the significance level as asterisks. Each significance level is associated to a symbol: *p*-values (0, 0.001, 0.01, 0.05, 0.1, 1) = symbols (“***”, “**”, “*”, “.”, " “).

Atmos. Chem. Phys. Discuss., https://doi.org/10.5194/acp-2017-613
Manuscript under review for journal Atmos. Chem. Phys.
Discussion started: 1 August 2017

Atmospheric Chemistry and Physics Discussions

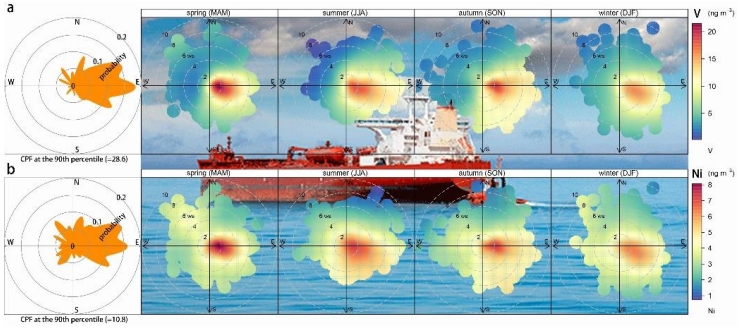

Figure 13. Conditional probability function analysis (left) and bivariate polar plots (right) of seasonal concentrations (ng m^{-3}) of V (**a**) and Ni (**b**) in Shanghai between March 2016 and February 2017. The center of each plot (centered at the sampling site) represents a wind speed of zero, which increases radially outward. The concentrations of V and Ni are shown by the color scale.

Atmos. Chem. Phys. Discuss., https://doi.org/10.5194/acp-2017-613
Manuscript under review for journal Atmos. Chem. Phys.
Discussion started: 1 August 2017

Atmospheric Chemistry and Physics Discussions

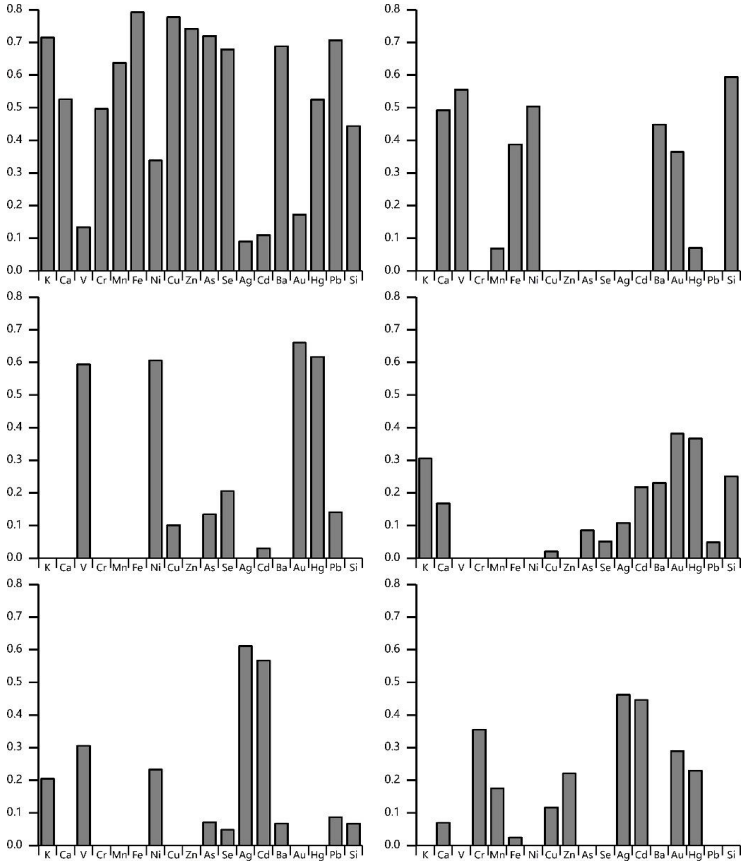

Figure 14. Principle component analysis of the 18 trace metals concentrations measured in Shanghai between March 2016 and February 2017. Six dominant factors are identified.

Atmos. Chem. Phys. Discuss., https://doi.org/10.5194/acp-2017-613
Manuscript under review for journal Atmos. Chem. Phys.
Discussion started: 1 August 2017

Atmospheric Chemistry and Physics Discussions

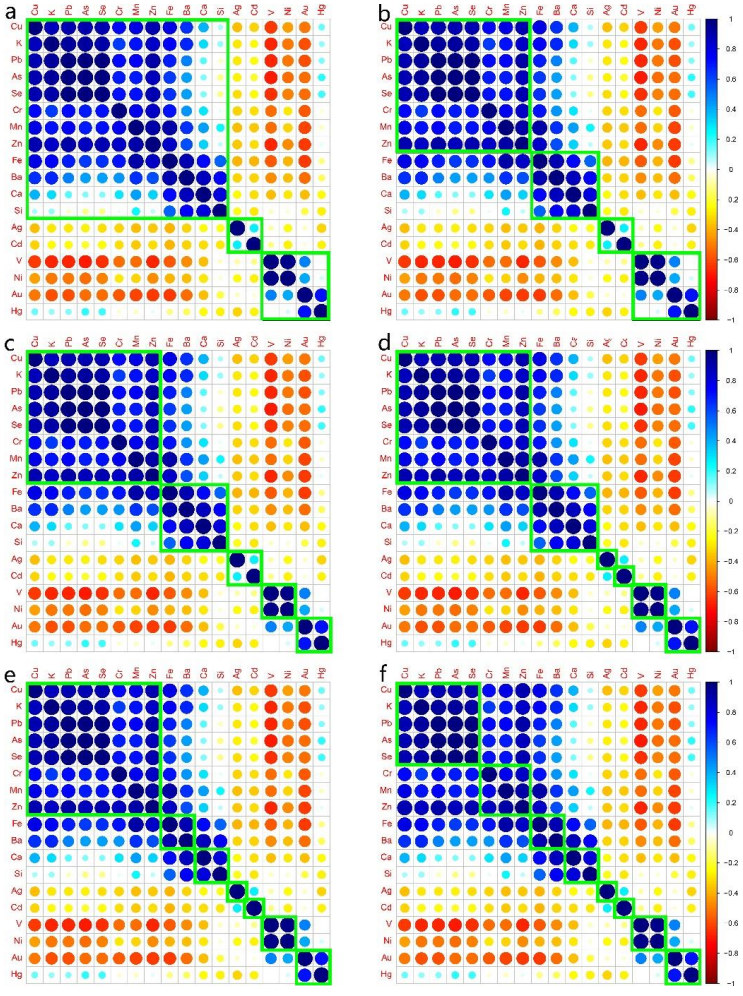

Figure 15. Hierarchical clustering orders of correlation matrix for the 18 trace elements measured in Shanghai between March 2016 and February 2017. Six solutions, from 3 factors to 8 factors, are shown from **a** to **f**.

Atmos. Chem. Phys. Discuss., https://doi.org/10.5194/acp-2017-613
Manuscript under review for journal Atmos. Chem. Phys.
Discussion started: 1 August 2017

Atmospheric Chemistry and Physics Discussions

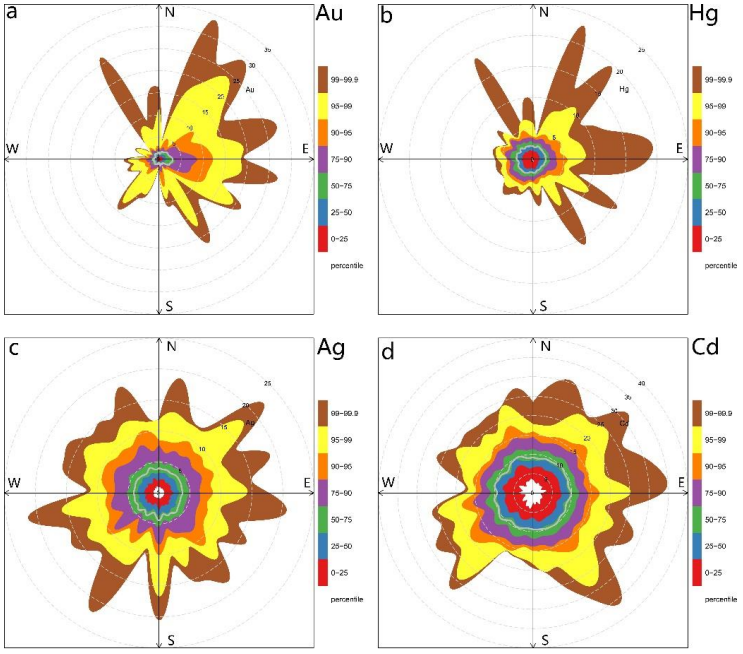

Figure 16. Percentile rose plot of Au (**a**), Hg (**b**), Ag (**c**), and Cd (**d**) concentrations in Shanghai between March 2016 and February 2017. The percentile intervals are shaded and shown by wind direction.

1215

1220

Atmos. Chem. Phys. Discuss., https://doi.org/10.5194/acp-2017-613
Manuscript under review for journal Atmos. Chem. Phys.
Discussion started: 1 August 2017

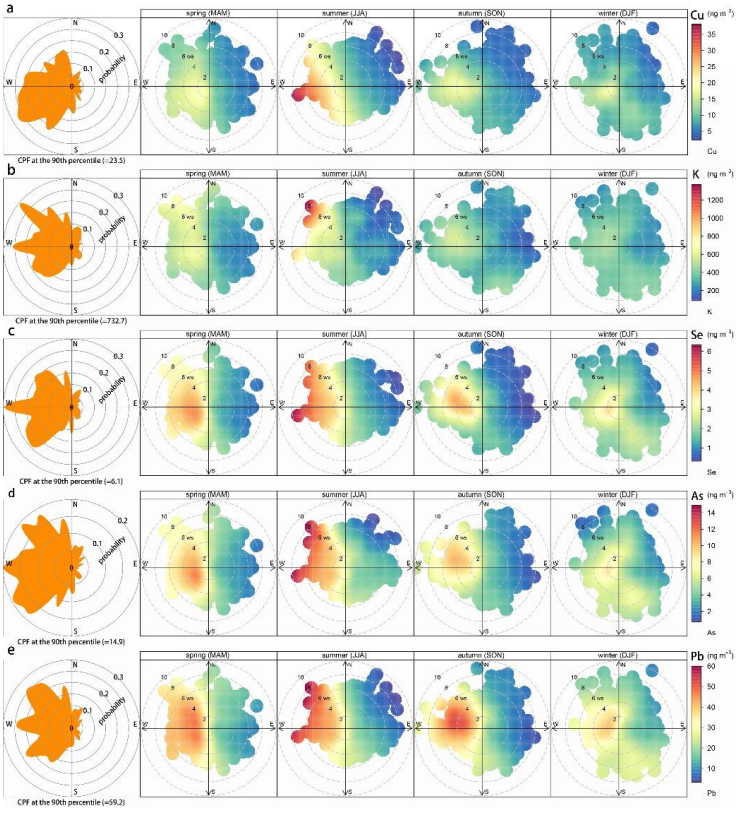

Figure 17. Conditional probability function analysis (left) and bivariate polar plots (right) of seasonal concentrations (ng m^{-3}) of Cu (**a**), K (**b**), Se (**c**), As (**d**), and Pb (**e**) in Shanghai between March 2016 and February 2017. The center of each plot (centered at the sampling site) represents a wind speed of zero, which increases radially outward. The concentrations of each species are shown by the color scale.